Molecular Dynamics
and
Free Energy Study
of Solubilization
# of solutes in SDS micelles

Kazushi FUJIMOTO

CONTENTS

I. General Introduction

A molecule consisting of hydrophilic group and hydrophobic group is called an amphiphilic molecule or a surfactant. Over the critical micellar concentration (CMC), the surfactants form aggregates where the hydrophobic group and the hydrophilic group of the surfactants are inside and outside the aggregates, respectively.[1] The aggregate is called “micelle”. In Japan the surfactant is produced one million tons a year, and the market scale is over ¥200 billion.

A water-insoluble substance can be dissolved in water because it penetrates into the micelle. This phenomenon is called “solubilization”.[1] The solubilization is utilized in various scientific or practical fields. For example, in pharmaceutics, a water-insoluble drug is dissolved and dispersed in water due to solubilization.[2] Furthermore, micelles with high affinity to diseased part of a patient is actively developed for drug delivery system.[3-5] In cosmetics, a water-insoluble perfume is also dissolved by using the micelle.[6-10] In synthetic chemistry, syntheses are often performed in the core of the micelle.[11, 12] Furthermore, in biochemistry, the solubilization of the proteins to the micelle is applied to extract membrane proteins from cells.[13-15] Now, more physicochemical studies of interaction between the micelle and the solubilized (= penetrating) molecules is necessary in order to have an insight into the solubilization phenomena.

So far, the free energy of transfer of the penetrating molecule from water phase into the micelles, e.g. a series of alkanes (methane, ethane, n-propane, n-butane, n-pentane) from the water phase into SDS micelles, was obtained experimentally by measuring the bound fraction of the penetrating molecules in the micelles.[16-21] The free energy decreases as a function of the number of carbon atoms

of the alkanes with a decrement of 3.2 kJ mol^{-1} per one methylene group.[19]

The binding site of the various penetrating molecules with the micelles has also been obtained by X-ray scattering and NMR experiments.[7, 22-25] The X-ray scattering experiments clarified that the alkane molecule (n-pentane) penetrate into micelle, whereas polar compounds such as long alkyl chain alcohols (n-heptanol, n-octanol, and n-decanol) and amine (n- decylamine) are solubilized in palisade layer of micelles, forming mixed micelles.[22, 23 25] In recent years, the binding sites of practical perfume molecules (*d*-limonene (LN) and geraniol (GL)) were measured by X-ray small angle scattering experiment.[7] The hydrophobic LN is found in the micelle core, but the hydrophilic GL is solubilized in palisade layer of the micelle. The binding sites of the various penetrating molecules to micelles are clarified by a large number of X-ray experiments. In these studies, however, the model structure of micelle with the penetrating molecule is assumed in order to analysis the X-ray scattering data. ^{19}F-NMR measurement unveiled that methanol molecule slightly penetrates to the sodium 12, 12, 12-trifluorododecyl sulfate micelle, but the binding sites of it is not clarified.[24]

The binding sites and free energy of transfer of the penetrating molecule in the micelle may be roughly obtained by several experiments stated above. However, in order to obtain more detailed information on the binding sites and binding strength of the penetrating molecules, we must evaluated the intermolecular interaction between the penetrating molecules and the micelle in atomic-level. It is difficult to obtain such information by experiments. Theoretical studies can make a significant contribution.

Theoretically, the phase-separation model and the mass-action model are well known for the thermodynamic models of solubilization phenomena in the previous studies[1]. In the former, the micelle is regarded as an isolated phase (micellar phase) in bulk water, and solubilization of the penetrating is treated as the partitioning of a water-insoluble molecule in the micellar phase. On the other hand, in the mass-action model, solubilization is regarded as a chemical reaction between a water-insoluble substance and the micelle. These models are powerful tools for understanding the solubilization phenomenologically. However, these models have no way to quantatively predict the binding site or the binding strength of the various penetrating molecules according to their chemical characteristics. In order to overcome the lack of prediction, Molecular-Thermodynamic model is proposed by Blankschtein *et al.*, where the partial free energy is assigned to each functional group of the surfactant molecules and the penetrating molecules, so that the free energy of new surfactant or penetrating molecule can be calculated by summing up the partial free energy of each functional group of them.[26-28] The binding strength predicted by this model is in good agreement with experiments. However, this model is also phenomenological. We need to construct the predictive method based on the statistical mechanics and atomic-level intermolecular interactions.

In this viewpoint, molecular dynamics (MD) calculation is a powerful tool to study the micelle and the solubilization. So far, MD calculation has given various molecular pictures of micelles.[29-31] A theoretical study of solubilization has been performed by Matubayasi *et al.*, based on distribution function theory combined with MD calculations.[32] The free energy profile was evaluated for pe-

netration of methane, benzene, and methylbenzene. In our previous work, the free energy of transfer of a water molecule was calculated using thermodynamic integration methods combined with MD calculations.[33]

In this research, the binding site and the binding strength of the penetrating molecule to micelle are clarified from a molecular level using MD calculations based on the statistical mechanics and the intermolecular interactions. The thermodynamic stability of the penetrating molecules between the inside and outside of the micelles is evaluated by calculating the free energy difference of the penetrating molecules between them. Then, the free energy can be calculated by various statistical mechanical methods, i.e. energy representation method and free energy perturbation method. Except for numerical error, a thermodynamic integration method is a strict method and easily implemented in our MD program so that the method is adopted in this research.

The Sodium dodecyl sulfate (SDS) was adopted for our calculations since the aggregation number and CMC of the SDS was most frequently reported in the surfactant molecules, and the SDS is widely used in various industrial fields. Methane, ethane, butane, hexane, and octane molecules were adopted as the hydrophobic penetrating molecules, and water, methanol, octanol, methylamine, and octylamine as the hydrophilic penetrating molecules.

This paper is consisted of 7 parts.

In chapter II, calculation methods were described.

In chapter III, the free energy of transfer of methane, ethane, n-butane, n-hexane, and

n-octane molecules from water phase to SDS micelle was calculated to clarify the stability of alkanes in the SDS micelle with increasing the number of carbon atoms.

In chapter IV, the enthalpy and entropy difference of transfer of the series of alkanes was also calculated. The effect of the chain length of the alkanes to the entropy difference was discussed. In order to clarify the relationship between the binding site of alkanes and the chain lengths, the radial distribution of the alkanes from the center of mass of the micelle is also calculated.

In chapter V, the radial free energy profile for penetration of methane and water molecules was calculated to obtain the binding site and the binding strength. Then, the free energy was divided into four contributions, i.e., the hydrophobic parts and sulfate ions of SDS micelle, sodium ions, and solvate water, and the contribution of each site is discussed.

In chapter VI, the free energy of transfer of methylamine, octylamine, methanol, and octanol from water phase to SDS micelle was calculated in order to clarify the effect of polar group. To show the relationship between the binding sites and the polar groups, the radial distribution of the alkanes is also calculated.

We conclude in chapter VII.

REFERENCE

1. Y. Moroi, *Micelles Theoretical and Applied Aspects* (Plenum, New York, 1992).
2. M. J. Carcia-Celma in *Industrial Applications of Microemulsions*, Surfactant Science Series, edited by C. Solans and H. Kunieda (Marcel Dekker, New York) Vol.66 p.123.
3. M. Yokoyama, M. Miyauchi, N. Yamada, T. Okano, Y. Sakurai, K. Kataoka, and S. Inoue, Cancer Res., **50** 1693 (1990).
4. K. Kataoka, A. Harada, and Y. Nagasaki, Adv. Drug Delivery Rev., **47** 113 (2001).
5. H. Kuramochi, Y. Andoh, N. Yoshii, and S. Okazaki J. Phys. Chem. **113**, 15181 (2009).
6. H. Nakajima in *Industrial Applications of Microemulsions*, Surfactant Science Series, edited by C. Solans and H. Kunieda (Marcel Dekker, New York) Vol.66 p.175.
7. Md. H. Uddin, N. Kanei, and H. Kunieda Langmuir **16**, 6891 (2000).
8. Y. Tokuoka, H. Uchiyama, M. Abe, and K. Ogino, J. Colloid Interface Sci., **152**, 402 (1992).
9. Y. Tokuoka, H. Uchiyama, and M. Abe, J. Phys. Chem., **98**, 6167 (1992).
10. Y. Tokuoka, H. Uchiyama, M. Abe, and S. D. Christian, Langmuir, **11**, 725 (1995).
11. V. Pillai and D. O. Shah, in *Industrial Applications of Microemulsions*, Surfactant Science Series, edited by C. Solans and H. Kunieda (Marcel Dekker, New York) Vol.66 p.227.
12. M. A. López-Quintela, J. Quibén-Solla, and J. Rivas, in *Industrial Applications of Microemulsions*, Surfactant Science Series, edited by C. Solans and H. Kunieda (Marcel Dekker, New York) Vol.66 p.247.

13. D. L. Foster and R. H. Fillingame, J. Biol. Chem. **254**, 8230 (1979).

14. M. J. Newman, D. L. Foster, T. H. Wilson, and H. R. Kaback, J. Biol. Chem. **256**, 11804 (1981).

15. H. Itami, Y. Sakaki, T. Shimamoto, M. T. H. Hama, and T. Tsuchiya, J. Biochem. (Tokyo) **105**, 785 (1989).

16. D. G. Marangoni and J. C. T. Kwak Langumuir, **7**, 2083 (1991).

17. J. J. Galan, J. L. D. Castillo, A. Gonzalez-Perez, V. Fuentes-Vanquenz, and J. R. Rodriguez, J. Therm. Anal. Cal. **87**, 159 (2007).

18. S. Nakamura, L. Kobayashi, R. Tanaka, T. Isoda-Yamashita, K. Motomura, and Y. Moroi, Langmuir, **24**, 14 (2008).

19. A. Wishnia, J. Phys. Chem. **67**, 2079 (1963).

20. B. Han, G. Yang, H. Yan, Z. Li, R. K. Thomas, J. Penfold, R. K. Heenan, and D. C. Steytler, J. Colloid Interface Sci. **218**, 145 (1999).

21. M. Hai, B. Han, G. Yang, H. Yan, and Q. Han, Langmuir **15**, 1640 (1999).

22. R. W. Matton, R. S. Stearns, and W. D. Harkins, J. Chem. Phys. **16**, 644 (1948).

23. W. D. Harkins, R. W. Mattoon, and R. Mittelmann, J. Chem. Phys. **15**, 763 (1947).

24. J. H. Fendler and E. J. Fendler, *Catalysis in micellar and macromolecular systems* (Academic Press, New York, 1975).

25. T. Yoshida, S. Shindo, T. Oogaki, and K. Yamanaka, *Shinban Kaimenkasseizai handbook* (kougakutosho, Tokyo, 2000) (in Japanese.)

26. V. Srinivasan and D. Blankschtein, Langmuir, **19**, 9932 (2003).

27. B. C. Stephenson, K. Beers, and D. Blankschtein, Langmuir, **22**, 1500 (2006)

28. B. C. Stephenson, C. O. Rangel-Yagui, A. Pessoa Jr., L. C. Tavares, K. Beers, and D. Blankschtein, Langmuir, **22**, 1514 (2006).

29. K. Watanabe, M. Ferrario, and M. L. Klein, J. Phys. Chem. **92**, 819 (1988).

30. A. D. MacKerell Jr., J. Phys. Chem., **99**, 1846 (1995).

31. D. P. Tieleman, D. van der Spoel, and H. J. C. Berendsen, J. Phys. Chem. B, **104**, 6380 (2000).

32. N. Matubayasi, K. K. Liang, and M. Nakahara, J. Chem. Phys. **100**, 9025 (1994).

33. N. Yoshii and S. Okazaki, J. Chem. Phys.. **126**, 0960101 (2007).

34. D. Frenkel and B. Smit, *Understanding molecular simulation from algorithms to applications* 2ed (Academic Press San Diego 2002)

II Calculation Method

A. Free energy

1. Thermodynamic integration method

Now we consider a process that a system changes from state *i* to *j*. Let $G(\lambda_i)$ be the Gibbs free energy of the whole system, where λ_i is a parameter which defines the state *i* of the system. The Gibbs free energy difference ΔG between state *i* and *j* can be calculated by thermodynamics integration method as follows.

$$\begin{aligned} \Delta G &= G(\lambda_j) - G(\lambda_i) \\ &= \int_{\lambda_i}^{\lambda_j} \frac{\mathrm{d}G}{\mathrm{d}\lambda}\,\mathrm{d}\lambda \\ &= \int_{\lambda_i}^{\lambda_j} \left\langle \frac{\mathrm{d}V(\lambda)}{\mathrm{d}\lambda} \right\rangle_{\lambda} \mathrm{d}\lambda. \end{aligned} \tag{2.1}$$

where $V(\lambda)$ is a potential energy of the system which depends on the parameter λ. The ensemble average of a derivative $\left\langle \mathrm{d}V(\lambda)/\mathrm{d}\lambda \right\rangle_{\lambda}$ is obtained by MD calculation.

2. Free energy of transfer of solutes from water phase to SDS micelles

Free energy of transfer of a solute molecule from water phase in a micellar solution to the micelle core, $\Delta G_{\mathrm{w}\to\mathrm{m}}$, has been evaluated by

$$\Delta G_{\mathrm{w}\to\mathrm{m}} = \Delta G_{\mathrm{id}\to\mathrm{m}} - \Delta G_{\mathrm{id}\to\mathrm{w}}, \tag{2.2}$$

where $\Delta G_{\mathrm{id}\to\mathrm{m}}$ and $\Delta G_{\mathrm{id}\to\mathrm{w}}$ are free energy of transfer of the solute molecule from an ideal gas state to the micelle core and the one from the ideal gas to the water phase, respectively. Figure 2.1 shows this thermodynamic cycle. The value of $\Delta G_{\mathrm{id}\to\mathrm{m}}$ and $\Delta G_{\mathrm{id}\to\mathrm{w}}$ may be calculated by the standard thermodynamic integration method combined with molecular dynamics calculations.

Now, we consider a system composed of $N + 1$ molecules. The first N molecules constitute one spherical micelle in solution and the $(N + 1)$-th molecule is the solute molecule. Suppose that the

solute molecule interacts with the micelle molecules as well as the solvent water through a set of ordinary interaction functions with coupling parameters, $\boldsymbol{\lambda}$, such that the potential energy of the whole system, $V(\boldsymbol{r}^{N+1}; \boldsymbol{\lambda})$, may be written as,

$$V(\boldsymbol{r}^{N+1};\boldsymbol{\lambda}) = V_N(\boldsymbol{r}^N) + \Delta V(\boldsymbol{r}_{N+1}, \boldsymbol{r}^N;\boldsymbol{\lambda}) + V_{N+1}^{\text{intra}}, \tag{2.3}$$

where $V_N(\boldsymbol{r}^N)$, $\Delta V(\boldsymbol{r}_{N+1}, \boldsymbol{r}^N;\boldsymbol{\lambda})$, and V_{N+1}^{intra} represent the sum of intra- and intermolecular interactions over the first N molecules, the intermolecular interaction between the (N + 1)-the molecule and the rest of the N molecules, and the intramolecular interaction of the (N + 1)-th molecule, respectively. In the present study, a two-parameter formula by Zacharias *et al.*[1] was adopted for the intermolecular potential function between the (N + 1)-th solute molecule and the rest of N micelle and solvent water molecules,

$$\begin{aligned}\Delta V(\boldsymbol{r}_{N+1}, \boldsymbol{r}^N;\lambda_1,\lambda_2) = {} & \lambda_1 \sum_{i\in M^N} \sum_{j\in M_{N+1}} \frac{1}{4\pi\varepsilon_0}\frac{q_i q_j}{r_{ij}} \\ & + \lambda_2 \sum_{i\in M^N} \sum_{j\in M_{N+1}} \left\{ \frac{A_{ij}}{[r_{ij}^{\,2} + \delta(1-\lambda_2)]^6} - \frac{B_{ij}}{[r_{ij}^{\,2} + \delta(1-\lambda_2)]^3} \right\},\end{aligned} \tag{2.4}$$

where $i \in M^N$ represents the i-th atom in one of the N molecules and $j \in M_{N+1}$ the j-th atom in the (N + 1)-th molecule. ε_0 is the dielectric constant of vacuum, q_i and q_j are the point charges of the i-th and j-th atoms, respectively, and A_{ij} and B_{ij} are the Lennard-Jones parameters between the i-th and j-th atoms. δ is a parameter which prevents divergence of the Lennard-Jones potential caused by the overlap of the (N + 1)-th molecule with any of the other N molecules. Here, the value of δ was set to be 0.05 nm^2.

At $\lambda_1 = \lambda_2 = 0$, the ($N$ + 1)-th molecule does not interact with the other N molecules. Then,

the (N + 1)-the molecule can be regarded to form an ideal gas. On the other hand, at $\lambda_1 = \lambda_2 = 1$, the ($N$ + 1)-th molecule fully interacts with the rest of the whole system. Then, the free energy difference ΔG between the states at $\lambda_1 = \lambda_2 = 1$ and 0 can be calculated by Eq. (2.1).

$$\begin{aligned} \Delta G &= G(\lambda_1 = \lambda_2 = 1) - G(\lambda_1 = \lambda_2 = 0) \\ &= \int_C \left\{ \left\langle \frac{\partial V}{\partial \lambda_1} \right\rangle_{\lambda_1,\lambda_2} \mathrm{d}\lambda_1 + \left\langle \frac{\partial V}{\partial \lambda_2} \right\rangle_{\lambda_1,\lambda_2} \mathrm{d}\lambda_2 \right\}, \end{aligned} \tag{2.5}$$

where $< \cdots >_{\lambda_1,\lambda_2}$ denotes the isothermal-isobaric ensemble average at fixed λ_1 and λ_2, and C is an integration path from $\lambda_1 = \lambda_2 = 0$ to $\lambda_1 = \lambda_2 = 1$. Integrands of Eq.(2.5) may easily be evaluated by ordinary molecule dynamics calculations

The integration path C in Eq. (2.5) may be chosen arbitrarily under the condition that the starting and ending terminal points are fixed at $\lambda_1 = \lambda_2 = 0$ and 1, respectively. In chapter III and VI, the integral paths C were chosen

$$\begin{aligned} \Delta G = &\int_0^{0.3} \left\langle \frac{\partial V}{\partial \lambda_2} \right\rangle_{\lambda_1\lambda_2} \mathrm{d}\lambda_2 \\ &+ \int_0^1 \left[\left\langle \frac{\partial V}{\partial \lambda_1} \right\rangle_{\lambda_1\lambda_2} + 0.7 \left\langle \frac{\partial V}{\partial \lambda_2} \right\rangle_{\lambda_1\lambda_2} \right] \mathrm{d}\lambda_1, \end{aligned} \tag{2.6}$$

and

$$\begin{aligned} \Delta G = &\int_0^{0.5} \left\langle \frac{\partial V}{\partial \lambda_2} \right\rangle_{\lambda_1\lambda_2} \mathrm{d}\lambda_2 \\ &+ \int_0^1 \left[\left\langle \frac{\partial V}{\partial \lambda_1} \right\rangle_{\lambda_1\lambda_2} + 0.5 \left\langle \frac{\partial V}{\partial \lambda_2} \right\rangle_{\lambda_1\lambda_2} \right] \mathrm{d}\lambda_1, \end{aligned} \tag{2.7}$$

respectively. In order to evaluate $\Delta G_{\mathrm{id}\to\mathrm{m}}$ and $\Delta G_{\mathrm{id}\to\mathrm{w}}$ separately by the thermodynamic integration method, integration space for the solute molecule of interest must be divided into the water phase and the micelle core. We defined that the solute is in the micelle where the distance from the center of

mass of the micelle to that of the solute is shorter than the radius of the micelle R_{m} = 2.8 nm, i.e., the average distance from the center of mass of the micelle to the interface between the micelle and water. When the distance is longer than R_{m}, the solute is considered to be located in the water phase.

Suppose that the spaces of the micelle core and the water phase are represented by the volume $V_{\mathrm{m}}\left(=\frac{4}{3}\pi R_{\mathrm{m}}^3\right)$ and $V_{\mathrm{w}}(=V-V_{\mathrm{m}})$, respectively, where V is volume of the MD box. Then, excess free energy of transfer of the solute from an ideal gas to the water phase $\Delta G^{\mathrm{ex}}_{\mathrm{id}\to\mathrm{w}}$ and to the micelle core $\Delta G^{\mathrm{ex}}_{\mathrm{id}\to\mathrm{m}}$ may be calculated by

$$\Delta G^{\mathrm{ex}}_{\mathrm{id}\to\mathrm{w}} = \Delta G(\boldsymbol{r}_{N+1}\in V_{\mathrm{w}}), \tag{2.8}$$

$$\Delta G^{\mathrm{ex}}_{\mathrm{id}\to\mathrm{m}} = \Delta G(\boldsymbol{r}_{N+1}\in V_{\mathrm{m}}), \tag{2.9}$$

where $\Delta G(\boldsymbol{r}_{N+1}\in V_{\mathrm{w}})$ and $\Delta G(\boldsymbol{r}_{N+1}\in V_{\mathrm{m}})$ represent the free energy difference ΔG in Eq. (2.6) or (2.7) for which the sampling of the integrands is made for the location of the alkane $\boldsymbol{r}_{N+1}\in V_{\mathrm{w}}$ and $\boldsymbol{r}_{N+1}\in V_{\mathrm{m}}$, respectively.

Then, the total free energy of transfer $\Delta G_{\mathrm{id}\to\mathrm{w}}(=\Delta G^{\mathrm{id}}_{\mathrm{id}\to\mathrm{w}}+\Delta G^{\mathrm{ex}}_{\mathrm{id}\to\mathrm{w}})$ and $\Delta G_{\mathrm{id}\to\mathrm{m}}(=\Delta G^{\mathrm{id}}_{\mathrm{id}\to\mathrm{m}}+\Delta G^{\mathrm{ex}}_{\mathrm{id}\to\mathrm{m}})$ may be written as

$$\Delta G_{\mathrm{id}\to\mathrm{m}} = \Delta G^{\mathrm{ex}}_{\mathrm{id}\to\mathrm{w}} - k_B T\ln\frac{V_{\mathrm{w}}}{V}, \tag{2.10}$$

$$\Delta G_{\mathrm{id}\to\mathrm{m}} = \Delta G^{\mathrm{ex}}_{\mathrm{id}\to\mathrm{m}} - k_B T\ln\frac{V_{\mathrm{m}}}{V}. \tag{2.11}$$

Now, the total free energy of transfer $\Delta G_{\mathrm{w}\to\mathrm{m}}$ of the solute from the water phase to the micelle is of the form

$$\Delta G_{\mathrm{w}\to\mathrm{m}} = \Delta G^{\mathrm{ex}}_{\mathrm{w}\to\mathrm{m}} - k_B T\ln\frac{V_{\mathrm{m}}}{V_{\mathrm{w}}}, \tag{2.12}$$

where

$$\Delta G^{\mathrm{ex}}_{\mathrm{w}\to\mathrm{m}} = \Delta G^{\mathrm{ex}}_{\mathrm{id}\to\mathrm{m}} - \Delta G^{\mathrm{ex}}_{\mathrm{id}\to\mathrm{w}}. \tag{2.13}$$

Restriction on the space for solute molecule

In order to sample the integrands in Eqs. (2.6) and (2.7) efficiently, space for the solute molecule of interest must be restricted in the water phase or in the micelle during the MD calculations. In order to do so, we introduced soft core wall potential for the solute as

$$\varphi_{\mathrm{wall}}(R, R_{\mathrm{m}}; \lambda) = \lambda \frac{A}{[(R - R_{\mathrm{m}})^2 + \delta(1-\lambda)]^6}, \tag{2.14}$$

in chapter III and

$$\varphi_{\mathrm{wall}}(R, R_{\mathrm{m}}) = \frac{A}{(R - R_{\mathrm{m}})^{12}}, \tag{2.15}$$

in chapter VI, respectively, where R is the distance between the center of mass of the micelle and that of the alkane. R_{m} is the distance form the center of mass of the micelle to the wall, for which the radius of the micelle is adopted. A is the interaction parameter between the solute molecule and the wall, which was adopted to be the same as that for the oxygen atom of SDS. Here, λ in Eq. (2.14)was set to be the same as λ_2. Then $\lambda_1 = \lambda_2 = 0$, the solute can go through the wall freely to be anywhere in the simulation box, whereas at $\lambda_1 = \lambda_2 = 1$ the position of the solute is restricted in the micelle or in the water phase, being separated by the wall. This wall potential causes an extra free energy to the system. However, this is very small such that it may be neglected in the present study.

3. *Free energy profile of solutes from water pahse to SDS micelles*

In chapter V we consider the transfer process of the methane or water molecule from a position in the water phase far from a micelle to the micelle core. The system is composed of an SDS micelle in water and one methane or water molecule to be examined. Here, the methane and water mole-

cules are called “solubilized” or “penetrating” molecules. Let r be the distance between the center of mass of the penetrating molecule and that of the SDS micelle, and let $G(r)$ be the Gibbs free energy of the whole system, where the distance is constrained to r. The Gibbs free energy of transfer $\Delta G(r)$ of the penetrating molecule from a reference distance r_0 to r may be calculated as[3-5]

$$\begin{aligned}\Delta G(r) &= G(r) - G(r_0) \\ &= \int_{r_0}^{r} \left(\frac{\mathrm{d}G(r')}{\mathrm{d}r'} \right) \mathrm{d}r' \\ &= \int_{r_0}^{r} \left\langle \frac{\partial \mathrm{V}}{\partial r'} \right\rangle_{r=r'} \mathrm{d}r' \\ &= \int_{r_0}^{r} \left\langle F(r') \right\rangle \mathrm{d}r',\end{aligned} \tag{2.16}$$

where $F(r')$ is the force acting between the center of mass of the SDS micelle and that of the penetrating molecule, separated by a distance r', and <···> represents the isothermal–isobaric ensemble average. $F(r')$ can be calculated as

$$F(r') = \left(\sum_{i \in M_\mathrm{s}} \frac{m_\mathrm{m}}{m_\mathrm{s} + m_\mathrm{m}} \boldsymbol{F}_i - \sum_{j \in M_\mathrm{m}} \frac{m_\mathrm{s}}{m_\mathrm{s} + m_\mathrm{m}} \boldsymbol{F}_j \right) \bullet \boldsymbol{u}, \tag{2.17}$$

where $\boldsymbol{F}_\mathrm{i}$ and $\boldsymbol{F}_\mathrm{j}$ are the forces acting on atom i and atom j, respectively, from all surrounding atoms, and m_s and m_m are the total masses of the penetrating molecule and the SDS micelle, respectively; $i \in M_\mathrm{s}$ and $j \in M_\mathrm{m}$ represent the i-th atom in the penetrating molecule and the j-th atom in the SDS micelle, respectively; and $\boldsymbol{u}$ is the unit vector from the center of mass of the penetrating molecule to that of the SDS micelle. The free energy profile can be evaluated from Eq. (2.16) using <$F(r')$> calculated from the MD.

B. Enthalpy and entropy

Enthalpy of transfer of a solute molecule form water phase in the micellar solution to the micelle core, $\Delta H_{\mathrm{w}\to\mathrm{m}}$, has been evaluated by

$$\Delta H_{\mathrm{w}\to\mathrm{m}} = \left\langle H_\mathrm{m} \right\rangle - \left\langle H_\mathrm{w} \right\rangle, \tag{2.18}$$

where $\langle H_{\mathrm{m}} \rangle$ and $\langle H_{\mathrm{w}} \rangle$ are the enthalpy of the micelle solution where the solute is in the micelle and the one where the solute is in the water phase, respectively. The $\langle H_{\mathrm{m}} \rangle$ and $\langle H_{\mathrm{w}} \rangle$ have been evaluated by

$$\begin{aligned} \langle H_{\mathrm{m}} \rangle &= \langle U_{\mathrm{m}} \rangle - P_0 \langle V_{\mathrm{m}} \rangle, \\ \langle H_{\mathrm{w}} \rangle &= \langle U_{\mathrm{w}} \rangle - P_0 \langle V_{\mathrm{w}} \rangle, \end{aligned} \tag{2.19}$$

where $\langle U_{\mathrm{m}} \rangle$ and $\langle V_{\mathrm{m}} \rangle$ are the average of the total energy and volume of the system, respectively, in which the solute is in the micelle core. $\langle U_{\mathrm{w}} \rangle$ and $\langle V_{\mathrm{w}} \rangle$ are the ones where the solute is in the water phase. P_0 is the pressure controlled by the Andersen method[2], i.e. 0.1 MPa. $\langle U \rangle$ and $\langle V \rangle$ have been obtained by the molecular dynamics calculations.

Entropy has been calculated by subtracting the free energy calculated by Eq. (2.2) from the enthalpy by Eq. (2.18)

$$T\Delta S_{\mathrm{w}\to\mathrm{m}} = \Delta H_{\mathrm{w}\to\mathrm{m}} - \Delta G_{\mathrm{w}\to\mathrm{m}}. \tag{2.20}$$

Since the enthalpy change is very small compared with its original value, large statistics was needed to obtain a reliable value. In order to evaluate $\langle H_{\mathrm{w}} \rangle$, space for the solute molecule of interest must be restricted in the water phase. We use potential of Eq. (2.15).

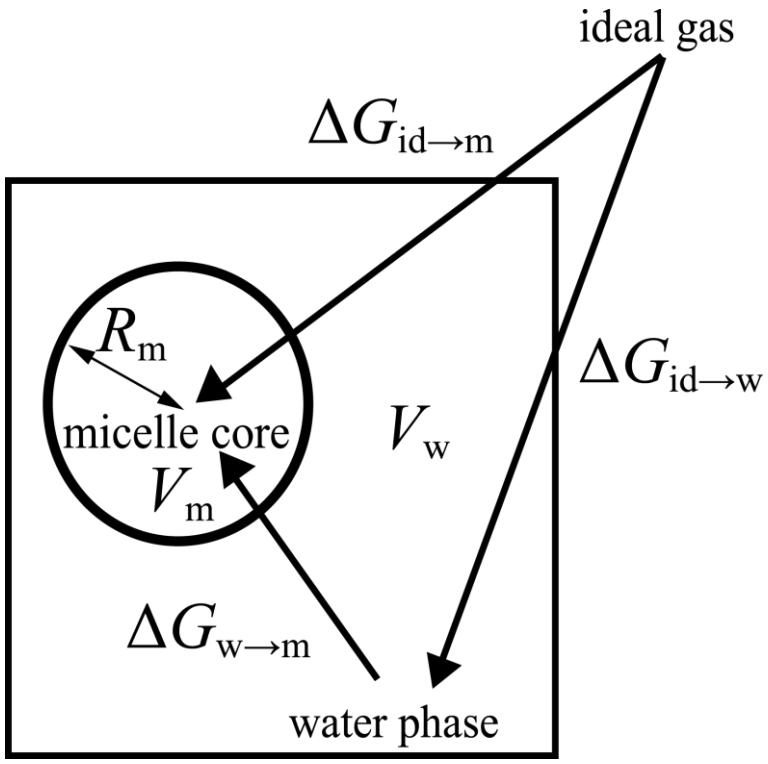

Fig. 2.1 Thermodynamic cycle for solubilization. Free energy of transfer of alkane from water phase to the micelle core, $\Delta G_{\mathrm{w}\rightarrow\mathrm{m}}$, may be calculated from the one from an ideal gas state to the water phase, $\Delta G_{\mathrm{id}\rightarrow\mathrm{w}}$, and the one from the ideal gas state to the micelle core, $\Delta G_{\mathrm{id}\rightarrow\mathrm{m}}$. R_{m} is the radius of the spherical micelle, and V_{m} and V_{w} are the volume of the micelle and the water phase, respectively.

REFERENCES

1. M. Zacharias, T. P. Straatsma, and J. A. McCammon, J. Chem. Phys. **100**, 9025 (1994).
2. D. Frenkel and B. Smit, *Understanding Molecular Simulation: From Algorithms to Applications*, 2nd ed. (Academic, New York, 2002).
3. S. Marrink and H. J. C. Berendsen, J. Phys. Chem., **98**, 4155 (1994).
4. W. Shinoda, M. Mikami, T. Baba, and M. Hato, J. Phys. Chem. B, **108**, 4155 (2004).
5. D. Bemporad, J. W. Essex, and C. Luttmann, J. Phys. Chem. B, **108**, 4875 (2004).

III. Molecular dynamics study of solubilization of immiscible solutes by a micelle: Free energy of transfer of alkanes from water to the micelle core by thermodynamics Integration method.

A. Introduction

In this chapter, the free energy of transfer of a series of hydrophobic solute molecules, i.e., methane, ethane, n-butane, n-hexane, and n-octane, from water phase to the micelle core has been calculated by thermodynamic integration method combined with molecular dynamics calculations in order to investigate the solubilization of immiscible solutes by the spherical SDS micelle. The calculated free energy is compared with the experimental one[1-3] as well as the theoretical one for methane by Matubayasi *et al.*[4] based on their distribution function theory in the energy representation.

B. Molecular dynamics calculations

Free energy of transfer from water phase to the SDS micelle core has been calculated by thermodynamic integration method combined with molecular dynamics calculations for methane, ethane, n-butane, n-pentane, and n-octane. In these calculations, the aggregation number of the SDS micelle was adopted to be 60 since our previous work[5] as well as the experiments[6, 7] showed that the aggregation number around 60 is thermodynamically most stable in the micellar solution. One alkane molecule, one spherical micelle, and 8,360 water molecules were contained in a cubic simulation box with the periodic boundary condition. The micelle concentration of the present SDS corresponds to about 50 CMC, i.e., about 10 wt%, where the SDS is found in the stable spherical micelle phase. CHARMM force field[8, 9] was used for the SDS and alkane molecules and TIP4P model[10] for water. The temperature and pressure were controlled at T = 300 K and P = 0.1 MPa, respectively, using the algorithm proposed by Martyna *et al.*[11, 12] Inertia of thermostat and barostat was set to be 3.0×10^{-12} and 0.5×10^{-12} s, respectively. The SHAKE/ROLL and RATTLE/ROLL algorithms were used to im-

pose the constraints on the bond lengths relevant to the hydrogen atoms.[12] Particle mesh Ewald (PME) method was adopted for the calculation of the long range interaction.[13] The Ewald dispersion parameter, α, was 0.375×10^{10} m^{-1} with the cutoff distance of 1 nm and the 128 × 128 × 128 grids for PME. The time step Δt was 1 fs. First, the molecular dynamics calculation was performed for 2 ns for equilibration of the micelle structure and spatial distribution of Na^+ ion. Then, in order to obtain sufficient statistics for the thermodynamic integration, molecular dynamics calculation was performed for 250–350 ps for each set of **λ**, for which the first 50 ps trajectory was excluded from the average.

During the MD calculations, location of the alkane molecule was monitored to decide at every step time whether it is in the water phase or in the micelle core according to the criterion described in the previous chapter. Following the decision, the integrand either for the alkane in the water phase or in the micelle core was summed up, respectively, see Eqs. (2.8) and (2.9). Here, we sampled the MD trajectories starting from two initial configurations. In one case, the alkane was located at $t = 0$ inside the wall, i.e., in the micelle, and, in the other case, it was set outside it, i.e., in the water phase. The former is to sample the configurations important for $\Delta G^{\mathrm{ex}}_{\mathrm{id}\to\mathrm{m}}$ efficiently and the latter is for $\Delta G^{\mathrm{ex}}_{\mathrm{id}\to\mathrm{w}}$.

Free energy of transfer $\Delta G^{\mathrm{ex}}_{\mathrm{id}\to\mathrm{pw}}$ of the alkanes from their ideal gas state to pure water has also been calculated in the same way as the case of the micelle solutions, where one alkane molecule was dissolved in 1,300 water molecules in the periodic boundary condition. In this case, the system is homogeneous such that no wall potential is needed.

C. Results and discussion

Figure 2.1 shows the time evolution of the first term of Eq. (2.6) for n-octane at $\lambda_1 = 0$ and $\lambda_1 = 0.5$. Since this alkane is the longest among the solute molecules studied in the present study and, further, the values of λ_1 and λ_2 are small, convergence of the cumulative average shown in the figure is expected to be slow compared with the other systems. As an example, ensemble averages of $\left\langle \partial V/\partial\lambda_2 \right\rangle_{\lambda_1,\lambda_2}$ and $\left\langle \partial V/\partial\lambda_1 \right\rangle_{\lambda_1,\lambda_2} + 0.7\left\langle \partial V/\partial\lambda_2 \right\rangle_{\lambda_1,\lambda_2}$ for n-octane transferring from the ideal gas state to the micelle core are presented for a series of (λ_1, λ_2) values in Fig. 2.2. The resultant $\Delta G^{\mathrm{ex}}_{\mathrm{id}\to\mathrm{m}}$ was -13 kJ mol^{-1}.

The error in $\Delta G^{\mathrm{ex}}_{\mathrm{id}\to\mathrm{m}}$ and $\Delta G^{\mathrm{ex}}_{\mathrm{id}\to\mathrm{w}}$ should be smaller than 3 kJ mol^{-1} in order to discuss, at least, the carbon number dependence of the free energy of transfer $\Delta G_{\mathrm{w}\to\mathrm{m}}$ of the alkanes from the water phase to the micelle core. However, average of the integrands over 200–300 ps in the present study might be too short to attain satisfactory statistics for the resultant $\Delta G_{\mathrm{id}\to\mathrm{m}}$ and $\Delta G^{\mathrm{ex}}_{\mathrm{id}\to\mathrm{w}}$. In order to test this, additional long-time MD calculations for 3.5 ns have been done for two conditions in Fig. 2.2, $\lambda_1 = 0$, $\lambda_2 = 0.025$ and $\lambda_1 = 0$, $\lambda_2 = 0.05$, for n-octane. The error of the integrand may be considered to be great for these two systems compared with the other conditions in the present study, i.e., the longest alkane and the smallest two λ_1 and λ_2's.

The average $\left\langle \partial V/\partial\lambda_2 \right\rangle_{\lambda_1,\lambda_2}$ from the 3.5 ns MD trajectory for $\lambda_1 = 0$ and $\lambda_2 = 0.025$ were 165 and 166 kJ mol^{-1} for n-octane molecule in the micelle core and in the water phase, respectively, the residence time being 0.75 and 2.75 ns, respectively. On the other hand, from the 300 ps trajectories, these were 154 and 167 kJ mol^{-1} for the former and for the latter, respectively. Thus, the differences

were 11 and 1 kJ mol^{-1}, respectively. For $\lambda_1 = 0$, $\lambda_2 = 0.05$, the differences were calculated to be 8 and 5 kJ mol^{-1} for the alkane in the micelle core and in the water phase, respectively. Thus, we can assume that the measure of the error in the calculated integrands in Fig. 2.2, for example, is, at most, 10 kJ mol^{-1} on average for $\lambda_2 \leq 0.1$. For $\lambda_2 > 0.1$, it can be assumed, at most, to be 5 kJ mol^{-1} since the value of the integrand itself is much smaller than that found for $\lambda_2 \leq 0.1$.

In the present case, the free energy difference we calculate is a summation of the integrands in Eq. (2.6) of the form $\Delta G = \sum_i \Delta\lambda_i \left\langle \partial V / \partial \lambda_i \right\rangle_{\lambda_i}$, the numerical integration, where, for simplicity, only one term is written. However, since the trajectories of the MD calculations with different λ_i are independent of each other, the calculated integrands may be considered to be independent of each other too. Then the error $\sigma_{\Delta G}$ included in ΔG must be $\sigma_{\Delta G}^2 = \sum_i \Delta\lambda_i^2 \sigma_{\lambda_i}^2$ where σ_{λ_i} is the error in the *i*-th integrand since the covariances are all zero. The estimated value of $\sigma_{\Delta G}$ following the above equation was as small as 2 kJ mol^{-1} even for the present very largely assumed values of σ_{λ_i}. The measure of σ_{λ_i} assumed in the present analysis, 10 kJ mol^{-1}, is presented by an arrow in Fig. 2.1. The figure clearly shows that the convergence of the cumulative average of the integrand is satisfactory based on the present 200–300 ps long MD calculation.

1. *Excess free energy of transfer*

Figure 2.3 shows the excess free energy of transfer from an ideal gas state to the water phase in the micellar solution, $\Delta G_{\mathrm{id}\rightarrow\mathrm{w}}^{\mathrm{ex}}$, and the one from the ideal gas state to the micelle core, $\Delta G_{\mathrm{id}\rightarrow\mathrm{m}}^{\mathrm{ex}}$, for a series of alkanes. It is found from the figure that $\Delta G_{\mathrm{id}\rightarrow\mathrm{m}}^{\mathrm{ex}}$ is smaller than $\Delta G_{\mathrm{id}\rightarrow\mathrm{w}}^{\mathrm{ex}}$ for all the alkanes from methane to n-octane. The alkanes are, thus, configurationally more stable in the micelle

core than in the water phase. Further, the value of $\Delta G^{ex}_{id\rightarrow m}$ decreases monotonically as a function of number of carbon atoms, n_c, and becomes negative for $n_c \geq 4$, at this micelle concentration, ~50 CMC, indicating that except for methane and ethane, the alkanes are thermodynamically more stable in the micelle than in the ideal gas state with the volume V. On the other hand, $\Delta G^{ex}_{id\rightarrow w}$ is positive for all the alkanes.

2. *Total free energy of transfer*

In Fig. 2.4, the calculated total free energy of transfer of the guest solute from water phase in the present micellar solution at 50 CMC to the micelle core, $\Delta G_{w\rightarrow m}$, calculated by Eq. (2.2) is plotted for each alkane together with the experimental value at 8 CMC (Refs. 1 and 2) and that at 5 CMC (Ref. 3) from the solubility measurement as well as the theoretical one[4] at 40 CMC based on the distribution function theory.

Comparison of the free energy of transfer at different micelle concentrations has been made by reducing the experimental and theoretical values to those at 50 CMC, i.e., by adding the correction term $-k_B T \ln V_w^{50CMC} / V_w^c$ to the experimental and theoretical free energies, where V_w^c represents the volume of the water phase at the concentrations adopted in the experiments and theory, respectively. Here, only the translational free energy of the alkane in the volume is taken into account assuming that the micelle concentration dependence of the configurational free energy of the dissolved alkane in the water phase may be neglected.

As clearly shown in the figure, the present study is in good agreement with both of the experiments and theory at the common micelle concentration, 50 CMC. Further, the figure clearly shows

that $\Delta G_{w\to m}$ decreases almost linearly as a function of n_C except for methane. The decrement of $\Delta G_{w\to m}$ per methylene group (–CH_2–) of the alkanes, $\partial\Delta G_{w\to m}/\partial n_C$, was evaluated to be −3.3 kJ mol^{-1} by the linear fitting of $\Delta G_{w\to m}$ for $2 \le n_c \le 8$. The value is also in very good agreement with the experiment, −3.2 kJ mol^{-1}.[1] The above agreement of the total free energy of transfer corrected for the different concentrations as the volume effect implies that the excess free energy of transfer without correction agrees well, too, among the present calculation, the experiments, and the theory.

The calculated free energy of transfer, $\Delta G_{id\to m}$ and $\Delta G_{id\to pw}$, from the ideal gas state with the volume V was corrected by adding $-k_B T \ln V_0/V$, where V_0 is the volume of the ideal gas at 0.1 MPa and 300 K, in order to obtain the free energy of transfer, $\Delta G_{id\to w}$ and $\Delta G_{id\to pw}$, from the ideal gas state at 0.1 MPa. In Fig. 2.5, the calculated total free energy of transfer from the ideal gas state at 0.1 MPa to the water phase in solution, $\Delta G_{id\to w}$, and to the pure water, $\Delta G_{id\to pw}$, calculated in this study is plotted for the alkanes together with the experimental free energy of transfer from the gas state at 0.1 MPa to pure water, $\Delta G_{g\to pw}$. First, the calculated $\Delta G_{id\to w}$ is in good agreement with the calculated $\Delta G_{id\to pw}$, and second, the calculated $\Delta G_{id\to w}$ as well as the $\Delta G_{id\to pw}$ is in good correspondence to the experimental $\Delta G_{g\to pw}$. The former means that the presence of Na^+ ion in the micellar solution has little influence on $\Delta G_{id\to w}$. This may be caused by the rather weak interaction between Na^+ and alkane.

All the values plotted in Fig. 2.5 are positive due to the instability of hydrophobic hydration of the alkanes. Furthermore, the hydration free energy has a minimum value for ethane both in the

calculation and experiment. Stability of the alkane in water may be related to the hydration or the cage formation by the solvent water molecules around it[14] since the cage structure itself clearly depends on the size of the alkane molecule. Thus, the present result indicates that the hydration structure of ethane is most stable among the alkanes studied here. Further, the carbon number dependence of $\Delta G_{\mathrm{id}\rightarrow\mathrm{w}}$ found in Fig. 2.5 is small compared with that of $\Delta G_{\mathrm{id}\rightarrow\mathrm{m}}$, see also Fig. 2.3. This implies that the free energy of transfer $\Delta G_{\mathrm{w}\rightarrow\mathrm{m}}$ in Fig. 2.4 is dominated by the dissolving process of the alkanes to the hydrophobic micelle core.

Free energy of transfer of methane and n-octane from the ideal gas state at 0.1 MPa to the micelle core and to the water phase in the micellar solution at the concentration of 50 CMC in the present calculation is illustrated in Fig. 2.6 as an energy level diagram. The result for the guest water molecule obtained in our previous study[5] is also presented in the figure.

For methane, $\Delta G_{\mathrm{id}\rightarrow\mathrm{m}}$ and $\Delta G_{\mathrm{id}\rightarrow\mathrm{w}}$ are 2 and 6 kJ mol^{-1}, respectively, showing that both processes are thermodynamically unfavorable. The instability is greater in water than in the micelle core. As a result, $\Delta G_{\mathrm{w}\rightarrow\mathrm{m}}$ has a negative value of − 4 kJ mol^{-1}. That is, the methane prefers moving from the water phase into the micelle core to staying in the water phase under the condition that the methane is in the micellar solution. Calculating the $\exp\left(-\Delta G_{\mathrm{w}\rightarrow\mathrm{m}} / RT\right)$, we can estimate the probability that the guest solute is found in the micelle core assuming that the only one solute is accommodated in the micelle core. The value of $\Delta G_{\mathrm{w}\rightarrow\mathrm{m}}$ indicates that five of six methane molecules are found in the micelle at T=300 K. On the other hand, for n-octane, $\Delta G_{\mathrm{id}\rightarrow\mathrm{m}}$ and $\Delta G_{\mathrm{id}\rightarrow\mathrm{w}}$ were eva-

luated to be − 15 and 11 kJ mol^{-1}, respectively. Here, it must be pointed out that the n-octane molecule is more stable in the micelle core than in the ideal gas state at 0.1 MPa although it is unstable in water. The combined effect gives the considerably negative $\Delta G_{w\rightarrow m}$ =− 26 kJ mol^{-1}, implying that almost all of the n-octane molecules are found in the micelle, only 1 of the 32,000 molecules being dissolved in the water phase. This may be understood by the concept of hydrophobicity too. Almost all the alkane molecules move from the water phase to the hydrophobic micelle core in order to avoid the contact with water molecules and reduce the hydrophobic hydration.

Here, it is interesting to compare the above findings with the case of the water molecule. In our previous work, the calculated $\Delta G_{w\rightarrow m}$ for water was + 28 kJ mol^{-1}. From this, we could evaluate that only 1 of the 75,000 water molecules is found inside the micelle core while the rest of the water molecules are free in the water phase. From the energetical point of view, water molecules do not like to cut their hydrogen bonds with other water molecules to move into the micelle core.

D. Conclusion

In order to evaluate the solubilization free energy of alkanes, i.e., methane, ethane, n-butane, n-hexane, and n-octane by the spherical SDS micelle, thermodynamic integration has been done executing the isobaric and isothermal molecular dynamics calculations for the micellar solution which contains a single alkane molecule. Negative free energy of transfer $\Delta G_{w\rightarrow m}$ from water phase to the micelle core was obtained for all the alkane molecules in the present study, which indicates that alkanes are more stable in the micelle core than in the water phase. Reflecting this negative free energy, the alkane molecules resided in the micelle core all the time during the calculation for a few nanose-

conds without wall potential.

The calculated free energy of transfer $\Delta G_{\mathrm{w}\to\mathrm{m}}$ decreases almost linearly as a function of number of carbon atoms of the alkanes. It decreases by 3.3 kJ mol^{-1} per methylene group for the alkanes longer than methane. The factor $\exp\ \Delta G_{\mathrm{w}\to\mathrm{m}} / k_B T$ at 300 K indicates that only 1 of the 32,000 n-octane molecules is dissolved in the water phase.

In the future work, the free energy of transfer of the second or third molecule as a solubilized solute can be also evaluated by thermodynamic integration method. When the number of solute increases, the micelle becomes emulsion.

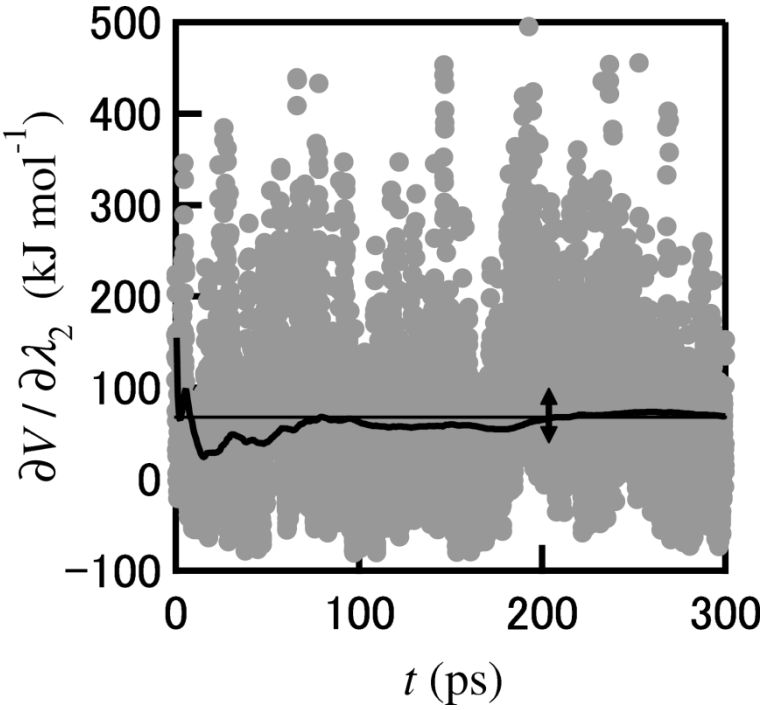

Fig. 2.1 An example of the calculated first term of Eq. (2.6) as a function of time (gray dots) for n-octane at $\lambda_1 = 0$, $\lambda_2 = 0.05$ as well as its cumulative average (black line). The arrow represents the tolerance of the error, 10 kJ mol^{-1}, which results in the error of 2 kJ mol^{-1} in the calculated free energy difference (see text).

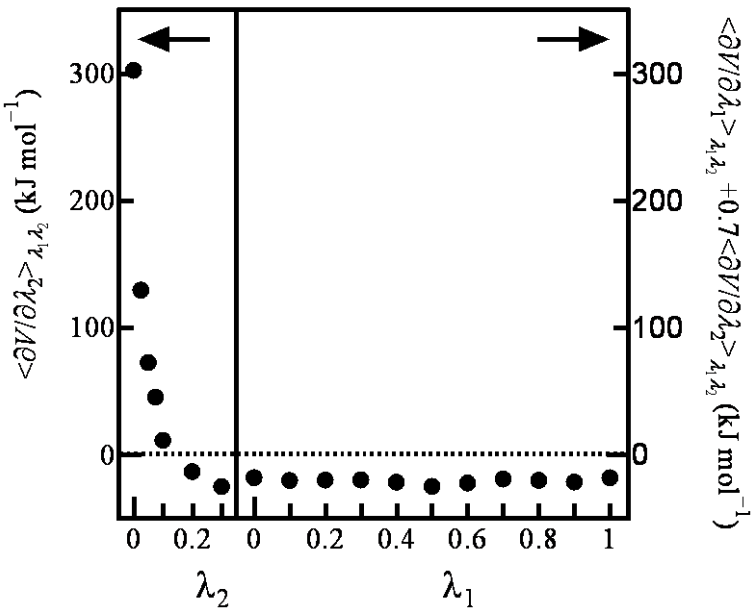

Fig. 2.2 The averaged $\langle \partial V/\partial \lambda_2 \rangle_{\lambda_1,\lambda_2}$ and $\langle \partial V/\partial \lambda_1 \rangle_{\lambda_1,\lambda_2} + 0.7\langle \partial V/\partial \lambda_2 \rangle_{\lambda_1,\lambda_2}$, the integrants of the thermodynamic integration method in Eq. (2.6), for n-octane transferred from the ideal gas state to the micelle core.

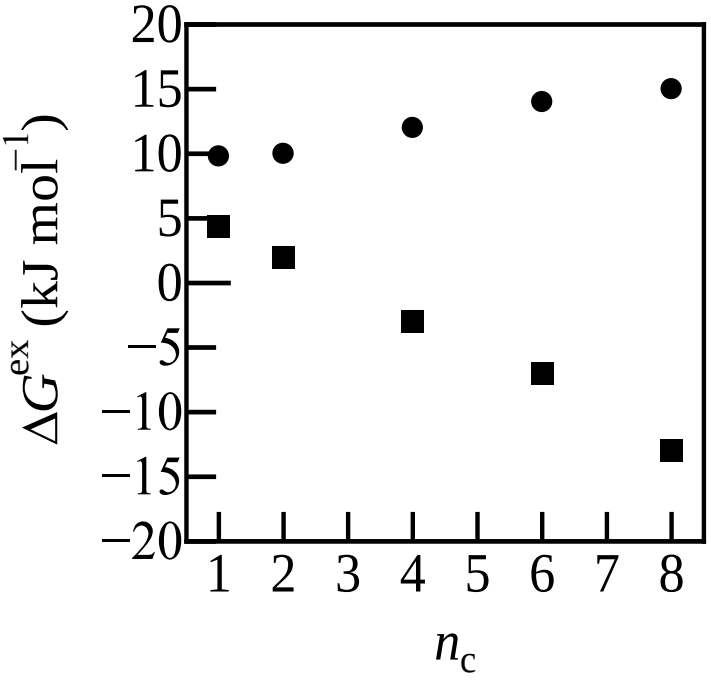

Fig. 2.3 The calculated excess free energy of transfer from an ideal gas state with the volume *V* to the water phase of the micellar solution (●) at 50 CMC and from the ideal gas to the micelle core(■) as a function of number of carbon atoms, n_c.

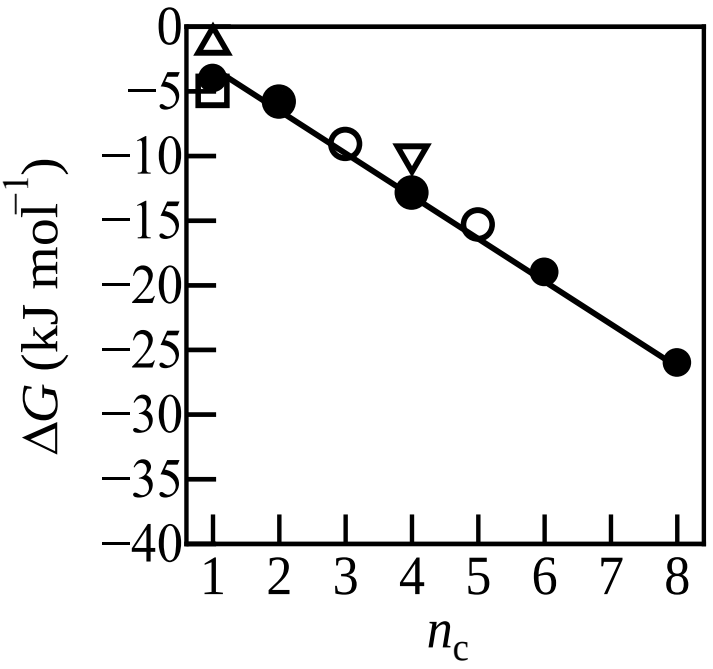

Fig. 2.4 The calculated total free energy of transfer from the water phase of the micellar solution to the micelle core. (●) Present study, (□) theory by Matubayasi *et al*. (Ref.4), and [(○), (△), and (▽)] experiments by Wishnia (Ref. 1), Han *et al*. (Ref. 2), and Hai *et al*. (Ref. 3), respectively.

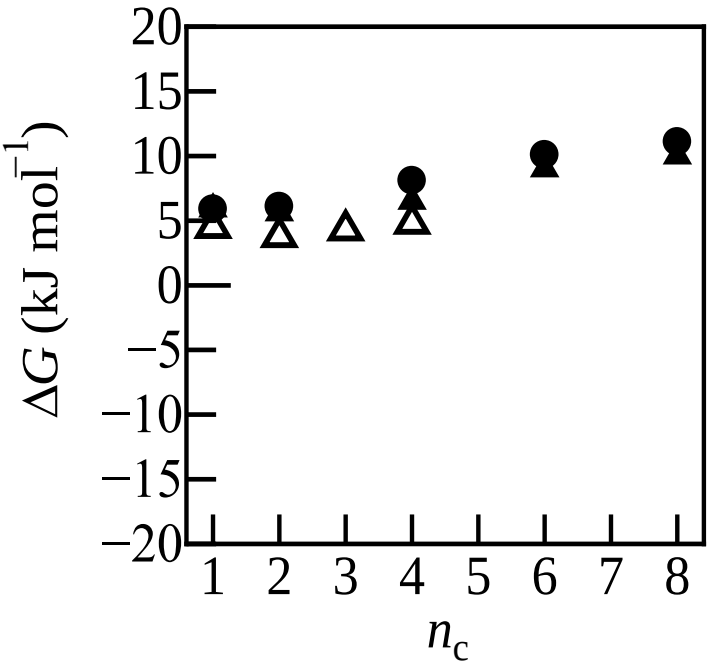

Fig. 2.5 The calculated total free energy of transfer from the ideal gas state at 0.1 MPa to the water phase of the micellar solution at 50 CMC (●) and from the ideal gas state to pure water (▲) compared with the experimental one (△) from the gas state to pure water (Ref. 15).

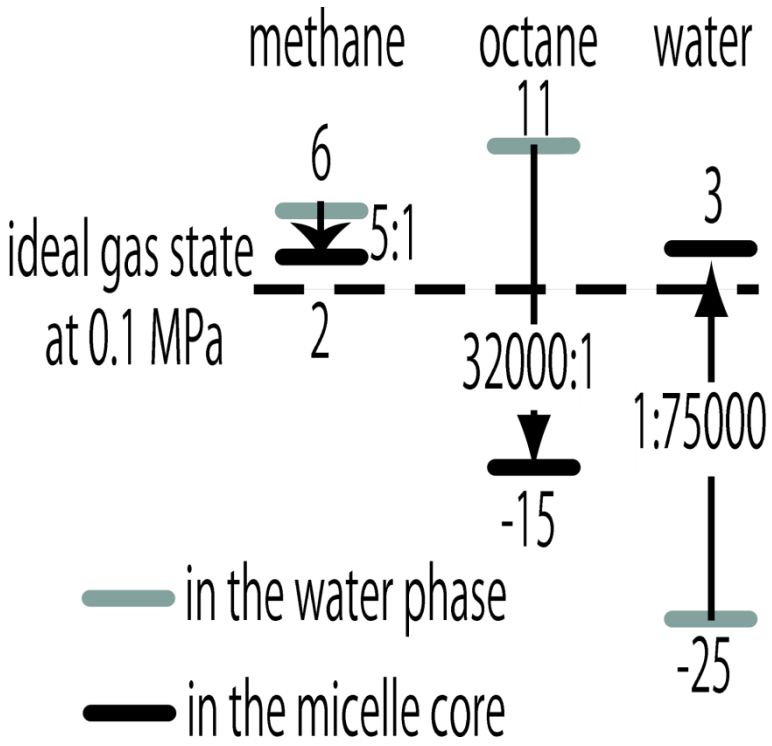

Fig. 2.6 The calculated free energy level for methane, n-octane, and water molecules in the ideal gas at 0.1 MPa, in the water phase of the micellar solution at 50 CMC, and in the micelle core.

REFERENCES

1. A. Wishnia, J. Phys. Chem. **67**, 2079 (1963).

2. B. Han, G. Yang, H. Yan, Z. Li, R. K. Thomas, J. Penfold, R. K. Heenan, and D. C. Steytler, J. Colloid Interface Sci. **218**, 145 (1999).

3. M. Hai, B. Han, G. Yang, H. Yan, and Q. Han, Langmuir **15**, 1640 (1999).

4. N. Matubayasi, K. K. Liang, and M. Nakahara, J. Chem. Phys. **124**, 154908 (2006).

5. N. Yoshii and S. Okazaki, J. Chem. Phys. **126**, 096101 (2007).

6. P. Lianos and R. Zana, J. Colloid Interface Sci. **84**, 100 (1981).

7. K. J. Mysels and L. H. Princen, J. Phys. Chem. **63**, 1696 (1959).

8. A. D. MacKerell, Jr., D. Bashford, M. Bellott, R. L. Dunbrack, Jr., J. D. Evanseck, M. J. Field, S. Fischer, J. Gao, H. Guo, S. Ha, D. Joseph-McCarthy, L. Kuchnir, K. Kuczera, F. T. K. Lau, C. Mattos, S. Michnick, T. Ngo, D. T. Nguyen, B. Prodhom, W. E. Reiher III, B. Roux, M. Schlenkrich, J. C. Smith, R. Stote, J. Straub, M. Watanabe, J. Wiórkiewicz-Kuczera, D. Yin, and M. Karplus, J. Phys. Chem. B **102**, 3586 (1998).

9. A. D. MacKerell, Jr., M. Feig, and C. L. Brooks III, J. Comput. Chem. **25**, 1400 (2004).

10. W. L. Jorgensen, J. Chandrasekhar, J. D. Madura, R. W. Impey, and M. L. Klein, J. Chem. Phys. **79**, 926 (1983).

11. G. J. Martyna, M. E. Tuckerman, D. J. Tobias, and M. L. Klein, Mol. Phys. **87**, 1117 (1996).

12. G. J. Martyna, D. J. Tobias, and M. L. Klein, J. Chem. Phys. **101**, 4177 (1994).

13. D. Frenkel and B. Smit, *Understanding Molecular Simulation: From Algorithms to Applications*,

2nd ed. (Academic, New York, 2002).

14. S. Okazaki, K. Nakanishi, H. Touhara, N. Watanabe, and Y. Adachi, J. Chem. Phys. **74**, 5863 (1981).

15. S. Cabani, P. Gianni, V. Mollica, and L. Lepori, J. Solution Chem. **10**, 563 (1981).

IV. Enthalpy and Entropy of transfer of alkanes from water phase to the micelle core

A. Introduction

In chapter III, free energy of transfer of a series of alkanes i.e. methane, ethane, n-butane, n-pentane, and n-octane from water phase to the sodium dodecyl sulphate (SDS) micelle core has been calculated by thermodynamic integration method combined with molecular dynamics calculations. In this calculation, it was observed that the free energy of transfer decreases almost linearly with increasing number of carbon atoms of alkanes. The finding may be simply explained by hydrophobicity of the solutes.

In this chapter, free energy of transfer from water phase to the micelle core has been divided into contributions from enthalpy and entropy. In particular, the entropy change as a function of size of alkanes has been investigated in terms of spatial distribution of alkanes in the micelle core as well as their conformational behavior.

B. Molecular dynamics calculations

Enthalpy and entropy of transfer from water phase to the SDS micelle core have been calculated by molecular dynamics calculations for methane, ethane, n-butane, n-pentane, and n-octane. In these calculations, the aggregation number of the SDS micelle was adopted to be 60, since our previous work[1] as well as the experiments[2, 3] showed that the aggregation number around 60 is thermodynamically the most stable in the micellar solution. One alkane molecule, one spherical micelle, and 8,360 water molecules were contained in a cubic simulation box with periodic boundary condition. CHARMM force field[4, 5] was used for the SDS and alkane molecules and TIP4P model[6] for water. The temperature and pressure were controlled at T = 300 K and P = 0.1 MPa, respectively using the algo-

rithm proposed by Martyna *et al.*[7, 8] Inertia of thermostat and barostat was set to be 3.0×10^{-12} s and 0.5×10^{-12} s, respectively. The SHAKE/ROLL and RATTLE/ROLL algorithms were used to impose the constraints on the bond lengths relevant to the hydrogen atoms.[8] Particle Mesh Ewald (PME) method was adopted for the calculation of the long range interaction.[9] Ewald dispersion parameter, α, was set to be 0.375×10^{10} m^{-1}, with the cutoff distance of 1 nm and the $64 \times 64 \times 64$ grid for PME. The time step Δt was 2 fs. Molecular dynamics calculation was performed for 15 ns for each alkane, and the last 10 or 12 ns data was used for analysis.

C. Results and discussion

Figure 4.1 shows a cumulative average of the enthalpy, $\langle H_{\mathrm{m}} \rangle$, of ethane. It shows that the fluctuation of the cumulative average became small in 1 ns MD calculation. So, the average for 1 ns was assumed as independent measurement such that the total average has been obtained from 10 or 12 independent measurements.

1. *Enthalpy and entropy*

Figure 4.2 shows the enthalpy, $\Delta H_{\mathrm{w}\to\mathrm{m}}$, and entropy, $T\Delta S_{\mathrm{w}\to\mathrm{m}}$, of transfer of alkane from water phase to the micelle core. As shown in the figure, the statistical error is not small such that it is difficult to discuss the calculated enthalpy and entropy quantitatively. However, the calculated enthalpy and entropy decrease with increasing number of carbon atoms of alkane. It is in good correspondence to the experiments[6]. Thus, we may discuss them qualitatively. The decrease of the enthalpy and entropy can be explained by the spatial distribution of the alkanes in the solution and their intramolecular structures, as stated below.

Other than the method used in this chapter, the entropy may be evaluated using thermodynamics integration method or temperature dependence of the free energy. But the statistical error is considered to be very large in both cases. In order to reduce the error, longer MD calculation is needed. The statistical error of the entropy must be reduced to be less than 1/10 of the present result. To do so, the calculation must be done more than 100 times longer than the present case (i.e. 1.5 μs). However, it is quite difficult in the present computational capacity. More powerful computational technique should be developed for entropy calculation.

2. *Radial distribution of alkanes*

Density profiles of hydrophobic and hydrophilic groups of the SDS micelle are presented in Figure 4.3(a) as a function of radial distance from the centre of mass of the micelle. The functions are also plotted in Figure 4.3(b) for the various alkanes in the micelle. In Figure 4.3(a), low density region is found in the centre of the micelle. Further, Figure 4.3(b) shows that all alkanes except for methane are localized in this low density region near the centre of the micelle. The longer the solute alkane molecule is, the more localized its spatial distribution is in the micelle core. In contrast to this observation, the methane molecule is found everywhere in the micelle.

In order to investigate the difference in the behavior between the methane molecule and the other alkane molecules, spaces or cavities in the micelle core which can accommodate a small molecule were analyzed. Figure 4.4 shows the calculated density profile of the cavities with a diameter of 0.3 nm. As clearly shown in the figure, the cavities which can accommodate methane molecule (about 0.3 nm) but are not large enough for the propane, butane, etc., are distributed over the micelle core. It

is interesting to find that the shape of the distribution is similar to that for the methane molecule. Thus, the methane molecule may move around the micelle core passing through these cavities.

The restriction of the space for the solute molecule in the micelle core causes more negative entropy of transfer from water phase where solute molecule may move almost freely. This explains the decrease of $T\Delta S_{w\to m}$ shown in Figure 4.2 as a function of number of carbon atoms of the alkanes.

3. *Distribution of head to tail distance*

In order to investigate the relation between the solubilization of alkane molecules and their structural change, conformation of the alkanes was analyzed. The calculated distribution, $f(r)$, of the head to tail distance, *r*, is presented in Figure 4.5 for the n-octane molecule in the micelle and in the water phase. The figure clearly shows that the distribution has a sharp peak at r = 0.88 nm both in the micelle core and in the water phase and a broad peak is also found at r = 0.76−0.86 nm. From the conformational analysis, it is found that the former peak represents the all-trans straight conformation and the latter shows the structure where one of five dihedral angles is gauche.

Integrating the function over the peak at r = 0.88 nm, it is found that 17% of the n-octane molecules has the all-trans conformation in the micelle core while it is 14% in the water phase. Mole fraction of the all-trans conformation of the solute in the micelle is greater than that found in the water phase by 3%. Further, in the water phase, a small peak is found at r = 0.74 nm. This represents the structure where two dihedral angles have the gauche conformation. Thus, the n-octane molecule has a compact structure in water to reduce the contact with water by the hydrophobic interaction.

Thus, as clearly shown in Figure 4.5, the conformation of the long alkane is considerably

restricted in the micelle core compared with that in the water phase. This results in smaller entropy of the solute alkane in the micelle core than in water and, thus, the negative entropy of transfer $T\Delta S_{w\rightarrow m}$. However, for short alkane, conformational degree of freedom is small. This is clear when we consider methane molecule where no conformational degree of freedom is found. Thus, the shorter the solute molecule is, the smaller the conformational effect on the entropy of transfer from water phase to the micelle core, $T\Delta S_{w\rightarrow m}$. This explains well the findings for $T\Delta S_{w\rightarrow m}$ shown in Figure 4.2.

D. Conclusion

In order to evaluate the solubilization enthalpy and entropy of alkanes, i.e., methane, ethane, n-butane, n-hexane, and n-octane by the spherical SDS micelle, a series of molecular dynamics calculations have been done for the micellar solution which contains one alkane molecule. The calculations showed that both of them decrease as a function of number of carbons of the alkane.

Spatial distribution of the alkanes in the micelle core as well as its conformation has been analyzed. The calculated radial density profile of the alkanes from the centre of mass of the micelle shows that the long alkanes are localized near the centre of the micelle core. In contrast, the small methane moves to and from a number of vacancies distributed in the micelle. Further, the longer the alkane is, the more localize its spatial distribution is in the micelle core. Further, the alkane molecules have more compact conformation in the water phase to reduce the contact with water, resulting in a wide distribution. In the micelle core, however, n-octane, for example, has a stretched structure to fit the linear alkyl chain of dodecyl sulfate ion. Thus, the calculated spatial distribution of the solute alkanes in the micelle core as well as their calculated torsional distribution explains qualitatively well

the observed entropy of transfer form water phase to the micelle core, i.e. the longer the solute alkane is, the more negative the entropy of transfer is.

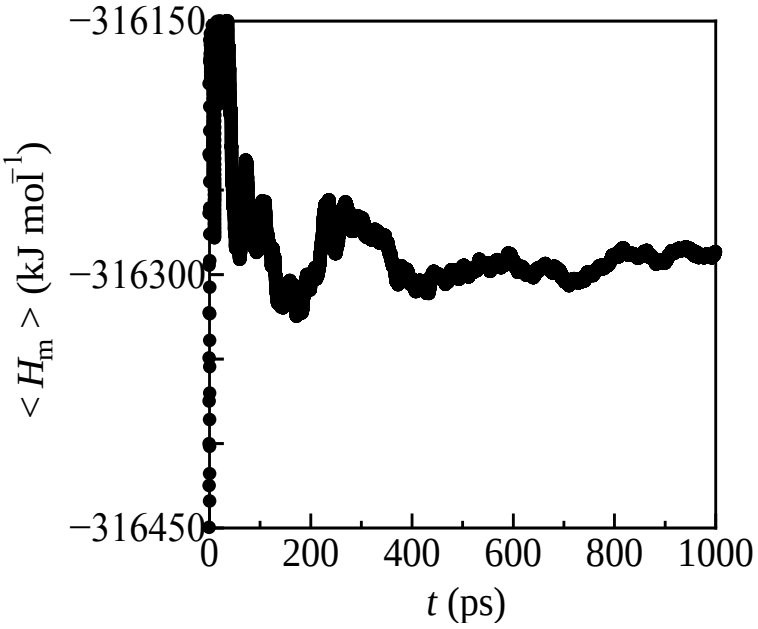

Fig. 4.1 The cumulative average of the enthalpy, $\langle H_{\mathrm{m}} \rangle$, of the micellar solution with ethane in the micelle core.

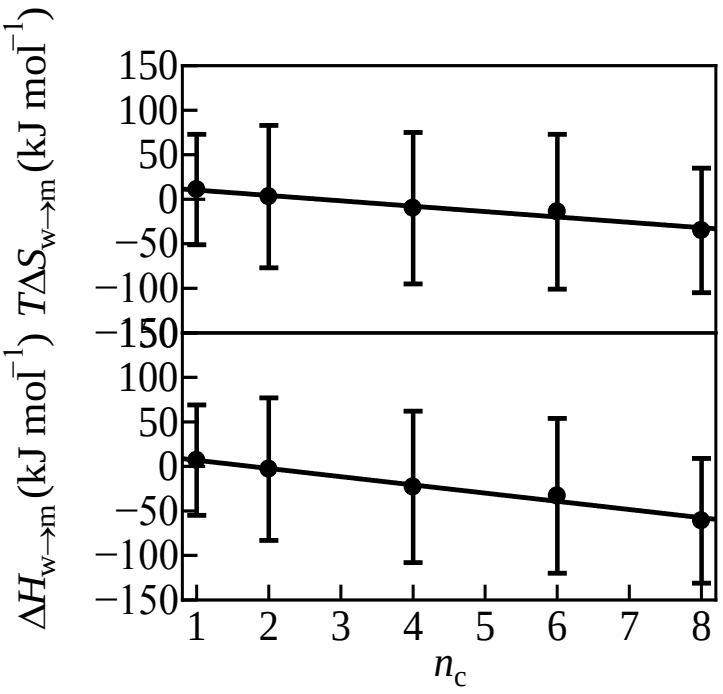

Fig 4.2 The calculated enthalpy, $\Delta H_{w\to m}$, and entropy, $T\Delta S_{w\to m}$, of transfer of the alkanes from water phase to the micelle core as a function of their number of carbon atoms, n_c. Error bars represent standard variation.

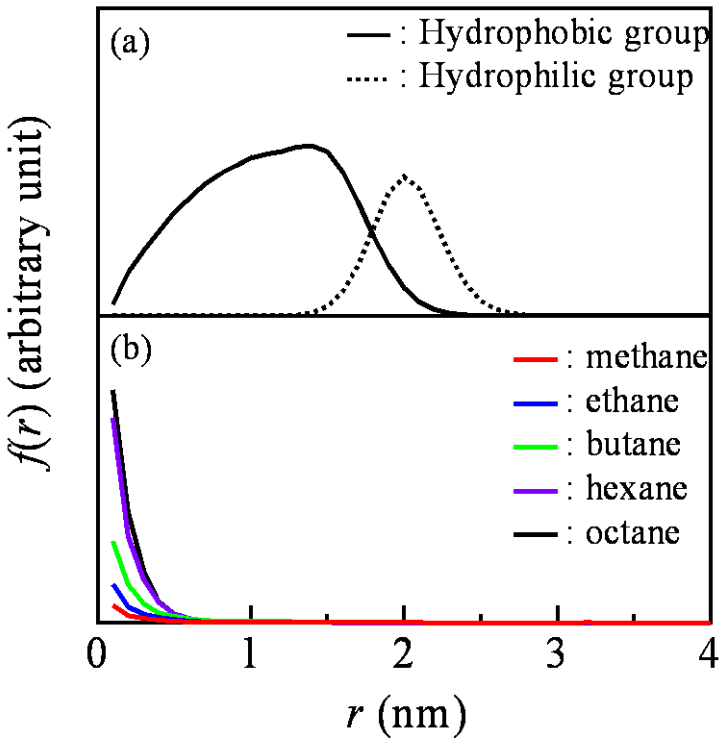

Fig. 4.3 The calculated density profile of (a) the hydrophobic group (—) and the hydrophilic group (---) of the micelle and (b) the carbon atoms of the solubilized alkanes, methane (—), ethane (—), n-butane (—), n-hexane (—), and n-octane (—) as a function of distance from the centre of mass of the micelle.

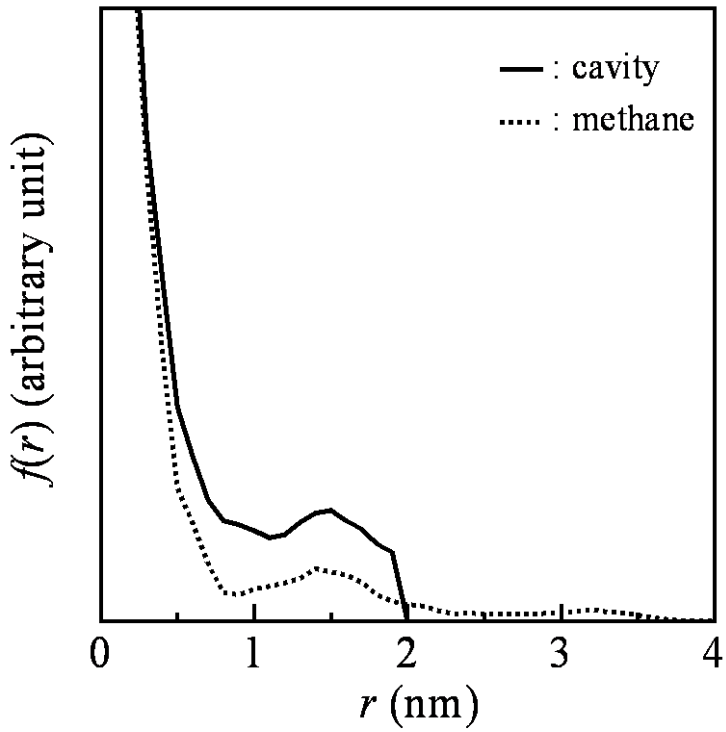

Fig. 4.4 The calculated density profile of cavities (—) with a diameter of 0.3 nm. The expanded plot of the spatial distribution of methane (---) is also presented.

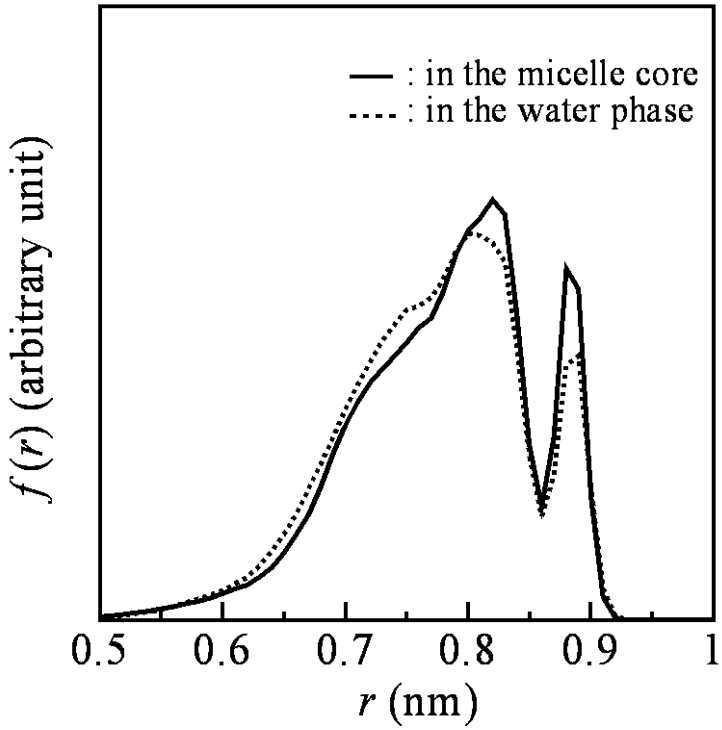

Fig. 4.5 The calculated distribution function of the distance between the head and tail carbons of n-octane in the micelle (—) and in pure water (---)

REFERENCES

1. M. J. García-Celma, *Solubilization of drugs in microemulsions* in *Industrial Applications of Microemulsions, surfactant science series, Vol. 66*, C. Solans and H. Kunieda, (Marcel Dekker, New York) p. 123.

2. M. J. Newman, D. L. Foster, T. H. Wilson, and H. R. Kaback, J. Biol. Chem. **256** 11804 (1981).

3. H. Itami, Y. Sakaki, T. Shimamoto, M. T. Hama, and T. Tsuchiya, J. Biochem. **105** 785 (1989).

4. V. Pillai and D. O. Shah, *Microemulsions as nanosize reactors for the synthesis of nanoparticles of advanced materials* in *Industrial Applications of Microemulsions, surfactant science series, Vol. 66*, C. Solans and H. Kunieda, (Marcel Dekker, New York) p. 227.

5. M. A. López-Quintela, J. Quibén-Solla, and J. Rivas, *Use of microemulsions in the production of nanostructured materials* in *Industrial Applications of Microemulsions, surfactant science series, Vol. 66*, C. Solans and H. Kunieda, (Marcel Dekker, New York) p. 247.

6. A. Wishnia, J. Phys. Chem. **67** 2079 (1963).

7. B. Han, G. Yang, H. Yan, Z. Li, R. K. Thomas, J. Penfold, R. K. Heenan, and D. C. Steytler, J. Colloid. Interfac. Sci. **218** 145 (1999).

8. M. Hai, B. Han, G. Yang, H. Yan, and Q. Han, Langmuir, **15** 1640 (1999).

9. N. Matubayasi, K. K. Liang, and M. Nakahara, J. Chem. Phys. **124** 154908 (2006).

10. K. Fujimoto, N. Yoshii, and S. Okazaki, J. Chem. Phys. **133** 074511 (2010).

11. N. Yoshii, K. Iwahashi, and S. Okazaki, J. Chem. Phys. **124** 184901 (2006).

12. P. Lanos and R. Zana, J. Colloid Interface Sci. **84** 100 (1981).

13. K.J. Mysels and L.H. Princen, J. Phys. Chem. **63** 1696 (1959).

14. A. D. MacKerell, Jr., D. Bashford, M. Bellott, R. L. Dunbrack, Jr., J. D. Evanseck, M. J. Field, S. Fischer, J. Gao, H. Guo, S. Ha, D. Joseph-McCarthy, L. Kuchnir, K. Kuczera, F. T. K. Lau, C. Mattos, S. Michnick, T. Ngo, D. T. Nguyen, B. Prodhom, W. E. Reiher III, B. Roux, M. Schlenkrich, J. C. Smith, R. Stote, J. Straub, M. Watanabe, J. Wiórkiewicz-Kuczera, D. Yin, and M. Karplus, J. Phys. Chem. B **102**, 3586 (1998).

15. A.D. MacKerell Jr., and M. Feig, and C.L. Brooks III, J. Comput. Chem. **25** 1400 (2004).

16. W.L. Jorgensen, J. Chandrasekhar, J.D. Madura, R.W. Impey, and M.L. Klein, J. Chem. Phys. **79** 926 (1983).

17. G.J. Martyna, D.J. Tobias, and M.L. Klein, J. Chem. Phys. **101** 4177 (1994).

18. G.J. Martyna, M.E. Tuckerman, D.J. Tobias, and M.L. Klein, Mol. Phys. **87** 1117 (1996).

19. D. Frenkel and B. Smit, *Understanding Molecular Simulation: From Algorithms to Applications* 2^{nd} *ed*., (Academic Press, New York, 2002).

V. Free energy profiles for penetration of methane and water molecules into spherical sodium dodecyl sulfate micelles obtained using the thermodynamic integration method combined with molecular dynamics calculations

A. Introduction

In this chapter, in order to clarify where the solubilized molecule is bound and how to stabilize it in the SDS micelle, the free energy profiles of penetration of hydrophobic methane and hydrophilic water have been calculated as a function of the distance between the center of mass of the SDS micelle and the penetrating molecule, using the thermodynamic integration method combined with MD calculations. The binding site and free energy barrier have been quantitatively evaluated. Furthermore, the solubilization free energy of the solubilized molecule was divided into four contributions, i.e., from the hydrophobic group, sulfate ions, sodium ions, and solvent water, in order to clarify which part of the solution is important. Finally, cavity distribution in the micelle was analyzed.

B. Molecular dynamics calculations

In the MD calculations, an aggregation number of 60 was adopted for the present SDS micelle since our previous work,[1] as well as light-scattering experiments[2, 3] and time-resolved fluorescence spectroscopy,[4] indicated that the aggregation number is thermodynamically most stable at about 60. Thus, 60 SDS molecules, 8,360 solvent water molecules, and one penetrating molecule (a methane or water molecule) were contained in a cubic simulation box with the periodic boundary condition. The SDS concentration in the present calculation is 50 CMC. TIP4P[5] and CHARMM[6, 7] potentials were used for water and the other molecules, respectively. It is noted that the polarization of water molecules near the micelle surface may be slightly different from that of bulk water because of the presence of the sulfate and sodium ions. In order to take such polarization effect of water into account, we can introduce high-cost polarizable model. However, in our previous free-energy study, fixed point charge model well reproduced the experimental aggregation number of SDS micelle. Thus, we believe that the fixed point charge TIP4P model is satisfactory for the present free-energy calculation. The pressure and temperature were controlled at P = 0.1 MPa and T = 300 K, using the algorithm proposed by Martyna *et al.*[8–10] The inertial constant of the barostat was set to 6.7×10^{-17} J s^2, so the relevant time constant is 2.0 ps. A five-fold Hoover chain thermostat was separately connected to particle degrees of freedom and the barostat. The inertial constants of the thermostat for the former were set to 3.6×10^{-21} J s^2 for the first chain and 1.2×10^{-21} J s^2 for the second to fifth chains, and those for the latter to 4.2×10^{-18} J s^2 for the first chain and 7.5×10^{-23} J s^2 for the second to fifth chains; the time

constants of the five chains are all 0.5 ps. The time step, Δt, was 2 fs. The particle mesh Ewald (PME)[11] method was adopted to calculate the Coulombic interaction. The cutoff distance for the Lennard-Jones interaction and the real-space part of the PME method was 1 nm. The parameter α and the grid points of the PME method were 0.4×10^{10} m^{-1} and $64 \times 64 \times 64$, respectively. SHAKE/ROLL and RATTLE/ROLL methods were used to constrain the bond length between carbon (C) and hydrogen (H) atoms in the methyl and methylene groups of dodecyl sulfate ions, the bond length between oxygen (O) and hydrogen atoms in the water molecule, and the bending angles H–C–H in the methylene groups and H–O–H in the water molecule.

2.1 *SDS micelle*

The initial configuration of the spherical SDS micelle was set such that the hydrophobic group of the dodecyl sulfate ion is inside the micelle and the hydrophilic sulfate ion is outside. Water molecules (8,360) were set around the SDS micelle in the simulation box. MD calculations were performed for 2 ns to equilibrate the micelle structure and spatial distribution of the sodium ions.

The initial configurations for the mean-force calculation were generated using the above equilibrated configuration of SDS micelles in water. A single penetrating molecule was located at a distance r from the center of mass of the SDS micelle. Here, the mean force $\langle F(r) \rangle$ was calculated at seven distances: r = 0.1, 0.5, 1.0, 1.5, 2.0, 2.5, and 3.0 nm. SHAKE and RATTLE methods were used to constrain the distance from the center of mass of the SDS micelle to that of the penetrating molecule. Each MD calculation was performed for 5 ns. The first 1-ns trajectory was excluded from the analysis. At r = 0.1 and 0.5 nm, MD calculations performed for 4 ns for the production run were sufficiently long to obtain the averaged value of $\langle F(r) \rangle$ because the trajectory of the penetrating molecule fully covers the whole spherical region of radius r, and satisfactory statistics were obtained from this. At r = 1.0, 1.5, 2.0, 2.5, and 3.0 nm, however, two MD calculations, starting from different initial configura-

tions, were performed at each distance to obtain enough statistics for analysis.

2.2 *Dodecane droplet*

In order to discuss differences between the penetration of the water molecule into the SDS micelle and the penetration of the water molecule into a hydrophobic droplet, as discussed in Section V.C, the free energy profile of water in a hydrophobic dodecane droplet has also been calculated. The aggregation number of the dodecane droplet was set to 60, as for the SDS micelle. One dodecane droplet, 8,397 water molecules, and one solubilized water molecule were contained in a cubic simulation box with the periodic boundary condition. TIP4P and CHARMM potentials were used for the water and dodecane molecules, respectively. The mean force $\langle F(r) \rangle$ was calculated at seven distances: r = 0.1, 0.5, 1.0, 1.5, 2.0, 2.5, and 3.0 nm. Each MD calculation was performed for 5 ns. The droplet, which is thermodynamically in the metastable state, was stable during these calculations. The first 1-ns trajectory was excluded from the statistics, and the remaining 4-ns trajectory was used for analysis. Details of the MD calculation were the same as those for the SDS micelles stated above.

C. Results and discussion

Figure 5.1(a) shows the calculated radial number density profile $\rho(r)$ of carbon atoms in the hydrophobic group, sulfur and oxygen atoms in the sulfate ion of the SDS micelles, solvent water molecules, and sodium ions. The $\rho(r)$ obtained in the present study is in very good agreement with the results of other studies.[12-14] For instance, the peak position of the sulfate ion of the SDS micelle is almost the same as that calculated by Matubayasi *et al*. Furthermore, as in the previous studies, a low-density region is observed at the center of the SDS micelle in the present work. These results in-

dicate that our calculations have been performed correctly.

1. *Mean force*

In Fig. 5.2, cumulative averages of $F(r)$ of solubilized methane (Fig. 5.2(a)) and water (Fig. 5.2(b)) molecules at r = 1.5 nm, evaluated using Eq. (2.17), are shown as a function of simulation time. The solid and dashed lines in Fig. 5.2(a) and (b) show the results of the MD calculations starting from two different initial configurations. At r = 1.5 nm, convergence is slowest among the various r values because of large fluctuations in $F(r)$ in the boundary region between the hydrophobic groups and sulfate ions of the SDS micelles. It was found that two cumulative averages converged to the same value $F(r = 1.5 \text{ nm}) = -2.0 \times 10^{-12}$ N for the methane and $F(r = 1.5 \text{ nm}) = 33 \times 10^{-12}$ N for the water after 4-ns MD calculations. The 4-ns MD calculations are therefore long enough to obtain satisfactory statistics for the mean force $\langle F(r) \rangle$. In order to evaluate the error of the mean force $\langle F(r) \rangle$, independent intervals were determined using the analysis of Fincham *et al.*[15] In this research, the time average of each 200-ps trajectory was regarded as an independent measurement of $F(r)$. Forty samples were obtained from two different 4-ns MD calculations at each distance of r = 1.0, 1.5, 2.0, 2.5, and 3.0 nm, and the statistical errors of $\langle F(r) \rangle$ were evaluated. At distances r = 0.5 and 0.1 nm, 20 samples were obtained from 4-ns MD calculations. The 80% confidence interval of $\langle F(r) \rangle$ was evaluated, and is shown by the error bar in Fig. 5.1.

Figure 5.1(b) shows the mean force $\langle F(r) \rangle$ of the solubilized methane and water molecules at distances r = 0.1, 0.5, 1.0, 1.5, 2.0, 2.5, and 3.0 nm. Positive values of $\langle F(r) \rangle$ indicate that the mean force acting on the solubilized molecule is a repulsive force, and excludes it from the SDS micelle. Negative values of $\langle F(r) \rangle$ indicate that the mean force acting on the solubilized molecule is an attractive force, and draws it into the SDS micelle. The figure shows that the interaction between methane and the SDS micelle is attractive at a range of $1.5 < r < 2.5$ nm, and that the interaction between water and the SDS micelle is repulsive at $0.5 < r < 2.0$ nm. At $0.1 \leq r \leq 0.5$ nm, attractive interactions can be

found for both methane and water. Details of the behavior are discussed in subsection V.C.3.

2. *Free energy profile for penetration*

Figure 5.1(c) shows the free energy profile $\Delta G(r)$ for penetration of methane and water. $\Delta G(r)$ can be obtained by integrating $\langle F(r) \rangle$ according to Eq.(2.16). In chapter II the free energy of transfer, ΔG, of the methane from bulk water to the SDS micelle core rather than the free energy profile $\Delta G(r)$ was calculated using the thermodynamic integration method with respect to the potential parameters. The free energy profile $\Delta G(r)$ for methane solubilization was also evaluated approximately by Matubayasi *et al*. using distribution function theory combined with MD calculations.[12] The results are also plotted in Fig. 1(c). $\Delta G(r)$ in the region of the SDS micelle ($0.1 \leq r \leq 1.5$ nm) is consistent with the value of $\Delta G(r) = -5$ kJ mol^{-1} and is in reasonable agreement with the $\Delta G(r)$ calculated by Matubayasi *et al*.

A free energy barrier is not observed between the micelle core and the bulk water, so methane can be easily solubilized into SDS micelles in the process of penetrating the micelle. The free energy in the SDS micelle core ($r = 0.1$ nm) is about 6 kJ mol^{-1} lower than in the hydrophilic part ($r =$ 1.2–2.5 nm). This indicates that from the viewpoint of excess free energy, the methane is more stable in the SDS micelle core than it is in the vicinity of the hydrophilic sulfate ions. However, the free energy difference (6 kJ mol^{-1}) between the micelle core and the hydrophilic part is not so large, only 2.4 times as large as the thermal energy at temperature $T = 300$ K. The solubilized methane might therefore be nonlocalized in the micelle core and move around in the whole of the micelle. Furthermore, the free energy difference between the hydrophilic part and the bulk water is also 6 kJ mol^{-1}, so the methane can easily go in and out of the SDS micelle. Distribution of the methane in the micelle will be discussed in more detail in subsection V.C.4.

With respect to the penetrating water molecule, a large positive $\Delta G(r)$ value around 24–35 kJ mol^{-1} is observed in the region $r \leq 1.0$ nm in Fig. 5.1(c). This value is in good agreement with the free energy of transfer of water from the water phase to the SDS micelle core of 28 ± 4 kJ mol^{-1} in our previous work.[22] It is certain that no water molecule permeates into the micelle core region in the present calculation (Fig. 5.1(a)), where $\Delta G(r)$ is larger than 10 kJ mol^{-1}.

The minimum $\Delta G(r)$ of methane and water is found at the center of the SDS micelle in the region r ≤ 0.5 nm. This feature is also observed in the free energy profile of a lipid membrane at the center of the membrane.[16-18] This phenomenon is commonly observed in the low-density region of the hydrophobic groups of surfactant and lipid molecules, i.e., the contact region of the tail end.

3. *Contributions from hydrophobic groups, sulfate ions, sodium ions, and solvent water to $\Delta G(r)$*

We clarify how hydrophobic groups and hydrophilic sulfate ions of SDS micelles, sodium ions, and solvent water affect the penetration of methane and water molecules into the SDS micelles. First, the force $F(r)$ acting on the penetrating methane and water was divided into contributions from the hydrophobic groups and sulfate ions of the SDS, sodium ions, and solvent water. When $\boldsymbol{F}_i$ and $\boldsymbol{F}_j$ in Eq. (2.17) are divided into these four contributions, $F(r)$ can be written as

$$\begin{aligned} F(r) = &\left(\sum_{i \in M_s} \frac{m_m}{m_s + m_m} \boldsymbol{F}^{pho}{}_i - \sum_{j \in M_m} \frac{m_s}{m_s + m_m} \boldsymbol{F}_j{}^{pho} \right) \bullet \boldsymbol{u} + \left(\sum_{i \in M_s} \frac{m_m}{m_s + m_m} \boldsymbol{F}^{phi}{}_i - \sum_{j \in M_m} \frac{m_s}{m_s + m_m} \boldsymbol{F}_j{}^{phi} \right) \bullet \boldsymbol{u} \\ &+ \left(\sum_{i \in M_s} \frac{m_m}{m_s + m_m} \boldsymbol{F}^{sod}{}_i - \sum_{j \in M_m} \frac{m_s}{m_s + m_m} \boldsymbol{F}_j{}^{sod} \right) \bullet \boldsymbol{u} + \left(\sum_{i \in M_s} \frac{m_m}{m_s + m_m} \boldsymbol{F}^{w}{}_i - \sum_{j \in M_m} \frac{m_s}{m_s + m_m} \boldsymbol{F}_j{}^{w} \right) \bullet \boldsymbol{u}, \end{aligned} \tag{5.1}$$

where the superscripts on $\boldsymbol{F}_i$, $\boldsymbol{F}_j$, i.e., pho, phi, sod, and w, stand for the hydrophobic groups and sulfate ions of the SDS, sodium ions, and solvent water, respectively. For example, $\boldsymbol{F}_i{}^{pho}$, found in the first term, represents the force acting on atom i of the penetrating methane or water from the hydrophobic groups of the SDS, and $\boldsymbol{F}_j{}^{pho}$ represents the force on atom j of the hydrophobic groups of the SDS from the penetrating methane or water. Thus, the first, second, third, and fourth terms in the right-hand side of Eq. (5.1) are the contributions to the mean force $\langle F(r) \rangle$ from the hydrophobic groups and sulfate ions of the SDS, sodium ions, and solvent water, respectively.

Formally integrating each contribution over r, we obtain a free energy-related quantity, whose summation gives the correct free energy. Of course, the quantity is not the thermodynamically defined free energy, but it works as a measure of the contribution to the free energy of interest. Here, we describe this quantity using the same symbol, $\Delta G(r)$, as that used for the free energy change. It should be noted that an infinite number of paths may exist in an actual penetrating process, taking

roundabout routes to the center of the micelle. However, in our analysis, the path dependence is averaged out and, at the same time, the force in only the r direction is investigated. Although contributions to the force acting on a penetrating molecule along an actual path are path dependent, we believe that the decomposition analysis in the present study is very useful in addressing the question of what role each component plays in the permeation.

Methane

In Fig. 5.3(a), the calculated mean force $\langle F(r) \rangle$ acting on the penetrating methane is shown with four contributions, i.e., from the hydrophobic groups and sulfate ions of the SDS micelle, sodium ions, and solvent water. The red and brown lines in Fig. 5.3(a) indicate that contributions from the sulfate ions and sodium ions are small in the whole region of r. This is because methane is a nonpolar molecule and interacts weakly with the sulfate ions and sodium ions. Even in the region $1.2 \leq r \leq 2.5$ nm, where the sulfate ions and sodium ions are largely distributed, contributions from the sulfate ions and sodium ions are quite small. The weak Lennard-Jones interactions between methane and the sulfate ions and sodium ions indicate that the methane is not in close contact with them. In contrast, contributions from the hydrophobic part and solvent water are dominant at r = 1.5 and 2.0 nm, the interface between the micelles and the water phase. Thus, contributions from the hydrophobic groups and solvent water are important for the solubilization of methane in the SDS micelle.

We now consider the solubilization of methane in the SDS micelle using the schematic diagram shown in Fig. 5.4. The number densities of the hydrophobic groups of the SDS micelle are represented by light and dark shades of gray; the darker the gray color, the higher the number density. Closed circles represent the methane molecules. The green and blue arrows indicate contributions to the mean forces $\langle F(r) \rangle$ on the methane from the interaction with the hydrophobic groups and solvent water, respectively. The inset in Fig. 5.4 shows the radial number density profile $\rho(r)$ of hydrophobic carbon atoms of the SDS micelle and solvent water.

At r = 3.0 and 2.5 nm in the water phase, only a very small force from the hydrophobic groups and solvent water was observed, as shown in Fig. 5.3(a). The small interaction between methane and the hydrophobic groups is simply a result of the distance between them, i.e., the Lennard-Jones force is short-range. The small averaged force from the solvent water, in spite of the close

contact, must be caused by symmetric hydration around the methane, which is located at a distance from the interface with the micelle. So, no arrow is drawn in Fig. 5.4. At r = 2.0 nm, however, an attractive force (blue arrow) acts on methane from the solvent water. A repulsive force from the hydrophobic groups is also acting on the methane (green arrow). However, as shown in Fig. 5.4, the attractive force is stronger than the repulsive one, so the methane is drawn into the SDS micelle. The attractive behavior of the total mean force in this interface region is, of course, caused by the hydrophobic interaction, which avoids the entropy loss of hydrophobic hydration of the methane. Here, we must remember that the hydrophobic interaction is a solvent-induced interaction, where water–water interactions play an essential role. Thus, in the present case, we should understand that, first, the solvent water molecules tend to gather together in order to reduce contact with the methane molecule located at the interface with the micelles. Secondly, this tendency is observed from the force on the methane from the water molecules (blue arrow), excluding it from the water phase. Thirdly, however, a small amount of work is required to push the methane molecule into the high-density region of the hydrophobic groups (green arrow). At r = 1.5 nm, the situation is similar to that at r = 2.0 nm, but the attractive and repulsive forces are balanced. At r = 1.0 nm, no contribution from solvent water is observed because the methane is not in contact with the solvent water at this distance, as shown in Fig. 5.1(a). With regard to the contribution from hydrophobic groups, almost no force is acting on the methane at r = 1.0 nm because the density gradient of the hydrophobic groups is small at that point, so the solvation structure may be considered to be symmetric. In the region where r < 1.0 nm, an attractive force associated with the hydrophobic part acts on the methane because of the lower density inside the SDS micelle.

Contributions to the free energy profiles were evaluated by integrating $\langle F(r) \rangle$ according to Eq.(2.16). The resulting profiles for four contributions are shown in Fig. 5.3(b). In this figure, contributions to the free energy profiles from the sulfate ions and sodium ions were found to be small, consistent with the results for the mean force $\langle F(r) \rangle$. The methane in the SDS micelle is stabilized by about 25 kJ mol^{-1} because of hydrophobic interaction induced by the solvent water, but it is destabilized by about 5–15 kJ mol^{-1} by the hydrophobic groups. Solubilization of methane into the SDS micelle therefore comes from avoidance of hydrophobic hydration of the methane.

Water

Figure 5.5(a) shows the contributions to the mean force acting on the penetrating water from hydrophobic groups, sulfate ions, sodium ions, and solvent water. These four contributions change in complex ways compared with the case of methane. The contributions from sulfate ions, sodium ions, and solvent water cancel one another. Thus, the total value becomes small, as shown in Fig. 5.5(a). This is also the case for the free energy profile shown in Fig. 5.5(b), where the contributions from sulfate ions, sodium ions, and solvent water to the free energy profile also cancel one another, and as a result, the total free energy change is small compared with the component changes.

In order to simplify the discussion, the mean force of water transfer to the dodecane droplet has also been calculated as a reference, using the thermodynamic integration method combined with MD calculations. The radial number density $\rho(r)$ of the hydrophobic groups of the dodecane and water molecules is presented in Fig. 5.6(a). Figure 5.6(b) shows the mean force between the water molecule and the dodecane droplet with two contributions to the mean force of penetrating water from the hydrophobic groups and solvent water. The calculated free energy profile $\Delta G(r)$, together with its two contributions relevant to the decomposition of the force in Fig. 5.6(b), is given in Fig. 5.6(c). First, we discuss this reference system before we investigate the micelle system of interest. It was found that at r = 1.0 and 1.5 nm, i.e., the interface region, a repulsive force acts on the water both from the hydrophobic groups and solvent water, resulting in the high free energy barrier found in Fig. 5.6(c). This result is consistent with the well-known view that a water molecule is less stable in a hydrophobic environment than in the water phase because of the energetic disadvantage of breaking the hydrogen-bonds formed in the water phase. This view may also be applied to the case of SDS, where a water molecule is unstable in the hydrophobic core of the micelle compared with in the water phase. The degrees of instability are similar to each other: 24–35 kJ mol^{-1} for SDS and 25 kJ mol^{-1} for the dodecane droplet. However, the behavior found at the interface region is very different. An essential difference between SDS micelles and dodecane droplets is the sulfate and sodium ions found in the interface region of the SDS micelles (see Fig. 5.1(a)). The radial distribution of ions shown in the figure forms a strong dipole moment at the interface, where sodium ions are widely distributed outside the location of sulfate ions. The structure of the solvent water must therefore be strongly influenced by this surface

dipole moment or the two ions. In fact, vibrational sum frequency generation (VSFG) spectroscopy shows that hydrogen atoms of water molecule near the interface of the SDS micelle are oriented toward the sulfate ion, and the hydrogen-bonding structure is different from that of the bulk water[19].

It is reasonable to consider that the force on a penetrating water molecule around the interface is dominated mostly by this dipole moment. The calculated mean forces shown in Fig. 5.5(a) may then be well understood as follows. At r = 3.0 nm, far from the interface, the mean forces acting on the penetrating water are all almost zero since the water molecule is in a symmetric field, as in bulk water. At r = 2.5 nm, near but outside the surface, forces from the solvent water and sodium ions cancel each other out. At r = 2.0 nm, at the interface, the forces from sulfate ions and sodium ions are great compared with the other components. Although the sign of their forces is different, as a result of the complicated structure of the interface, it is important to find that the two forces, about $+70 \times 10^{-12}$ N and -50×10^{-12} N from sulfate ions and sodium ions, respectively, or force from the dipole moments tend to keep the penetrating water molecules inside the water phase. The small negative force from the solvent water is no more than a secondary one after the ions at the surface have determined the structure, in particular, the orientation of the penetrating water molecule as well as the orientation of the solvent water molecules located across the ions. The orientations must be opposite, resulting in the negative force. At r = 1.5 nm, the dipole moment at the surface strongly draws the penetrating water back to the water phase, where the sign of the force is the same for sulfate ions and sodium ions. Furthermore, high-density hydrophobic tail-groups also tend to exclude the water molecule from the micelle core. Together with the counter-force from the solvent water, the total mean force on the water molecule is about 30×10^{-12} N, drawing it back to the water phase. At r = 1.0 nm, the situation is similar to the case at r = 1.5 nm, except for the values. At r = 0.5 nm and 0.1 nm, in the center of the hydrophobic core of the micelle, the averaged forces are small because of the long distance from the interacting groups or the symmetric force at a distance from the interface.

4. *Methane distribution in the SDS micelle solution*

The radial distribution $f(r)$ of methane from the center of mass of the SDS micelle may be evaluated by

$$f(r) \propto \exp(-\Delta G(r)/RT), \qquad (3.1)$$

where $\Delta G(r)$, R, and T are the free energy profile of methane as a function of r, the gas constant (R = 8.314 J mol^{-1}), and the absolute temperature, respectively. In Fig. 5.7, $f(r)$ is plotted together with $f_t(r)$, which is the radial distribution of methane evaluated from the 15-ns trajectory of MD calculations in our previous work. At r = 1.5 nm, $f_t(r)$ is reduced to the same value as $f(r)$. As shown in the figure, the shape of $f(r)$ is in good agreement with $f_t(r)$. The radial distribution $f_v(r)$ of the space that can accommodate a sphere of diameter of 0.3 nm, i.e., a cavity, in the micelle is also plotted in Fig. 5.7. $f_v(r)$ is also reduced to the same value as $f(r)$ at r = 1.5 nm. A good correlation between $f_v(r)$ and $f(r)$ indicates that both methane and cavities are distributed in the micelle, and the methane is considered to move about among the micelle cavities. As stated in subsection V.C.2, solubilized methane can come in and out through the surface of the micelle, so a distribution of methane can be seen outside the micelle at $r \geq 2.5$ nm in $f(r)$ and $f_t(r)$.

Both $f(r)$ and $f_t(r)$ show a high probability in the vicinity of the center of the micelle. The number of solubilized methane molecules can be calculated by multiplying the Jacobian $4\pi r^2$ and $f(r)$ together, as shown in the inset of Fig. 5.7. Although the error included in the value is large, we may qualitatively discuss the actual distribution of methane in the micelle. It is interesting to find that after the volume factor $4\pi r^2$ is taken into account, the methane is most often observed at the interface.

D. Conclusion

The free energy profiles $\Delta G(r)$ for penetration of methane and water molecules into SDS micelles have been calculated using the thermodynamic integration method combined with MD calculations.

Methane is about 6 kJ mol^{-1} more stable in the vicinity of the sulfate ions of the micelle than it is in the water phase. No free energy barrier is observed there, so the methane seems to be easily drawn into the micelle. Furthermore, methane in the center of the micelle is about 6 kJ mol^{-1} more stable than it is in the vicinity of the sulfate ions. The binding energy is about 2.4 times larger than the thermal fluctuation energy at T = 300 K. This value is relatively small, and therefore the solubilized methane may move about in the micelle core.

The relative contributions of the hydrophobic groups and sulfate ions of the SDS, sodium ions, and solvent water to methane solubilization in SDS micelles have been clarified. The contribu-

tions of solvent water and hydrophobic groups are dominant. With respect to the contribution from solvent water, in order to avoid hydrophobic hydration of methane in solvent water, the methane tends to be excluded from the water phase to the micelle. Considering the mean force just from the solvent water, the methane in the micelle is about 25 kJ mol^{-1} more stable than it is in the solvent water. In contrast, in the crowded hydrophobic groups of the micelle core, the methane is destabilized by 5–15 kJ mol^{-1} because of the repulsive interactions between methane and the hydrophobic groups. As a result, the methane remains in the micelle because the stability provided by the hydrophobic interaction is greater than the instability caused by the repulsive interactions between the methane and the hydrophobic parts.

The $\Delta G(r)$ of the penetrating water is evaluated to be 24–35 kJ mol^{-1}, so penetration of water into the micelle hardly occurs. The mean force $<F(r)>$ on the water was divided into four contributions. These contributions change in complex ways as a function of r, and cancel one another out. In order to solve this puzzle, we calculated the mean-force profile for transfer of water into the dodecane droplet as a reference, using MD calculations. The essential mechanism of the penetration of a water molecule is the same for the SDS micelle and the dodecane droplet; the water molecule is unstable in the hydrophobic core of the micelle and in the dodecane droplet compared with in the water phase. The complex behavior observed in the SDS micelle is from the strong dipole moment formed at the interface by sulfate ions and sodium ions.

Finally, the radial distribution of solubilized methane has been evaluated from $\exp\{-\Delta G(r)/RT\}$. A good correlation was found between the radial distribution of 0.3-nm cavities in the SDS micelle and that of the methane. The methane is considered not to be localized but to move about in the SDS micelle using cavities in the hydrophobic core.

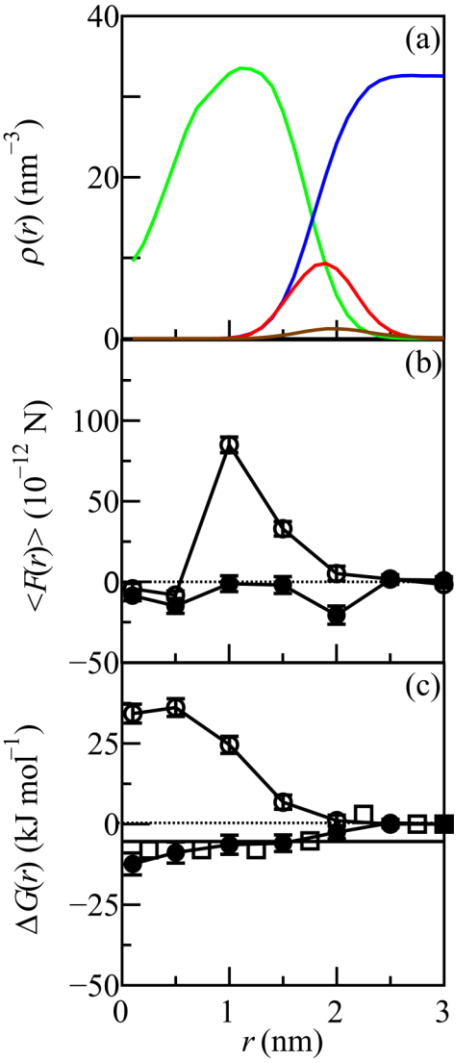

Fig. 5.1 (a) Radial number density profile $\rho(r)$ of SDS micelles as a function of radial distance from the center of mass of the SDS micelle (—: hydrophobic carbon atom, —: sulfur and oxygen atoms of sulfate ion, —: water molecule, and —: sodium ion), (b) the mean force $\langle F(r) \rangle$, and (c) the free energy profile $\Delta G(r)$ for penetration of a methane and a water molecule to the SDS micelle as a function of radial distance from the center of mass of the SDS micelle to those of penetrating methane and water molecules (●: methane and ○: water molecule). Open squares in Fig. 1(c) represent data obtained by Matubayasi *et al.*[12] Error bars in (b) and (c) represent 80% confidence intervals. See text for details.

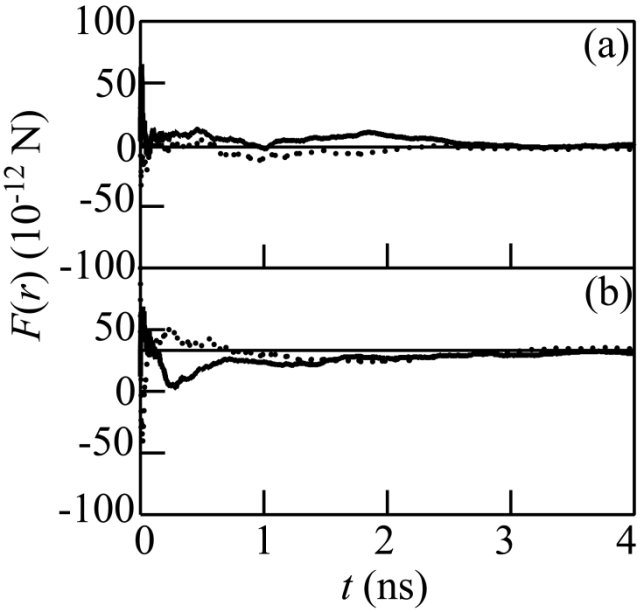

Fig. 5.2 Cumulative average of force $F(r)$ as a function of simulation time between SDS micelle and penetrating (a) methane and (b) water molecules at distance r = 1.5 nm. Solid and dashed lines are the results of MD calculations starting from two different initial configurations. Straight lines in (a) and (b) represent resultant averages of the mean force $\langle F(r) \rangle$.

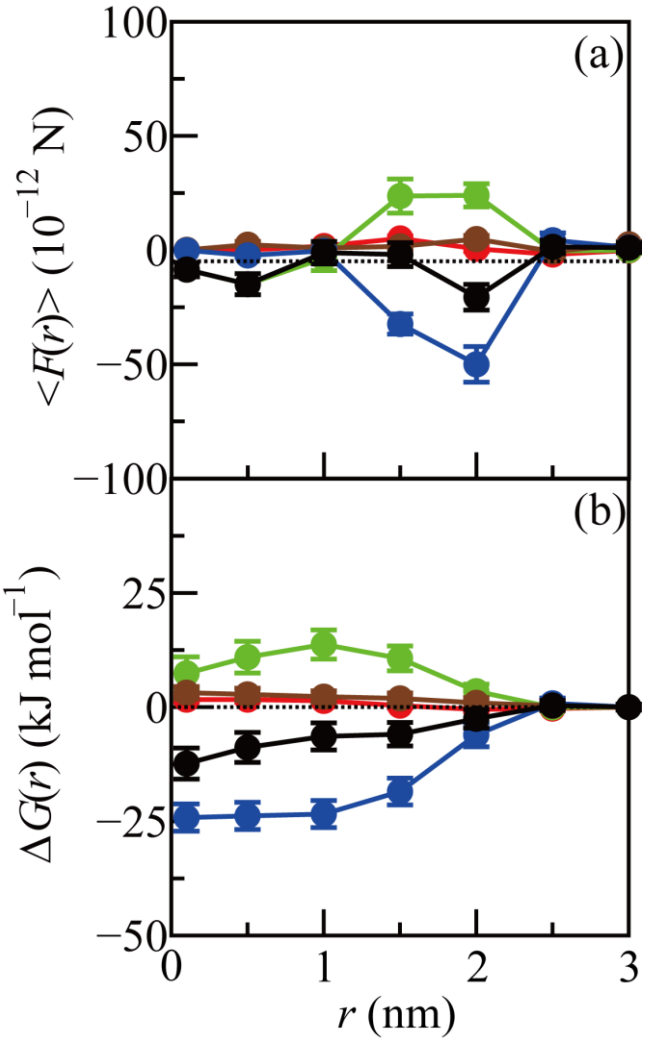

Fig. 5.3 Contributions from hydrophobic groups (●), sulfate ions (●), sodium ions (●), and solvent water (●) to (a) the mean force $\langle F(r) \rangle$ and (b) the free energy profile $\Delta G(r)$ for solubilization of methane molecules into SDS micelles. ● represents the total.

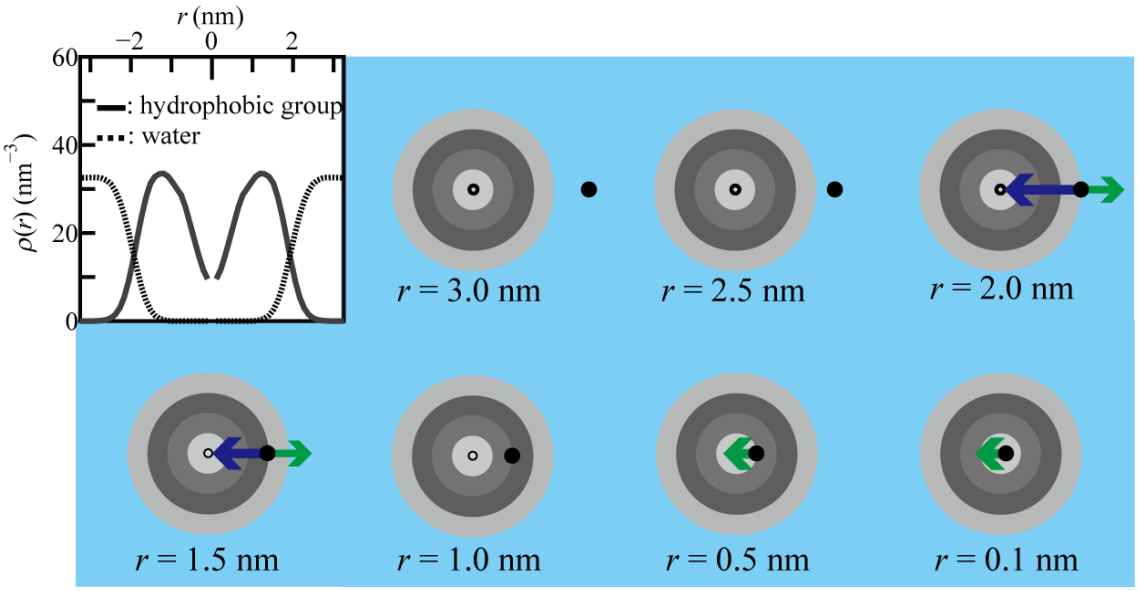

Fig. 5.4 Schematic diagram of solubilization of methane into SDS micelles. The inset shows the number density profile $\rho(r)$ of hydrophobic parts and water in SDS solution. The density of hydrophobic groups of SDS micelles is shown by shades of gray. Darker gray represents higher density. The black dot represents a methane molecule. The green and blue arrows represent mean forces $\langle F(r) \rangle$ arising from the hydrophobic groups and solvent water, respectively.

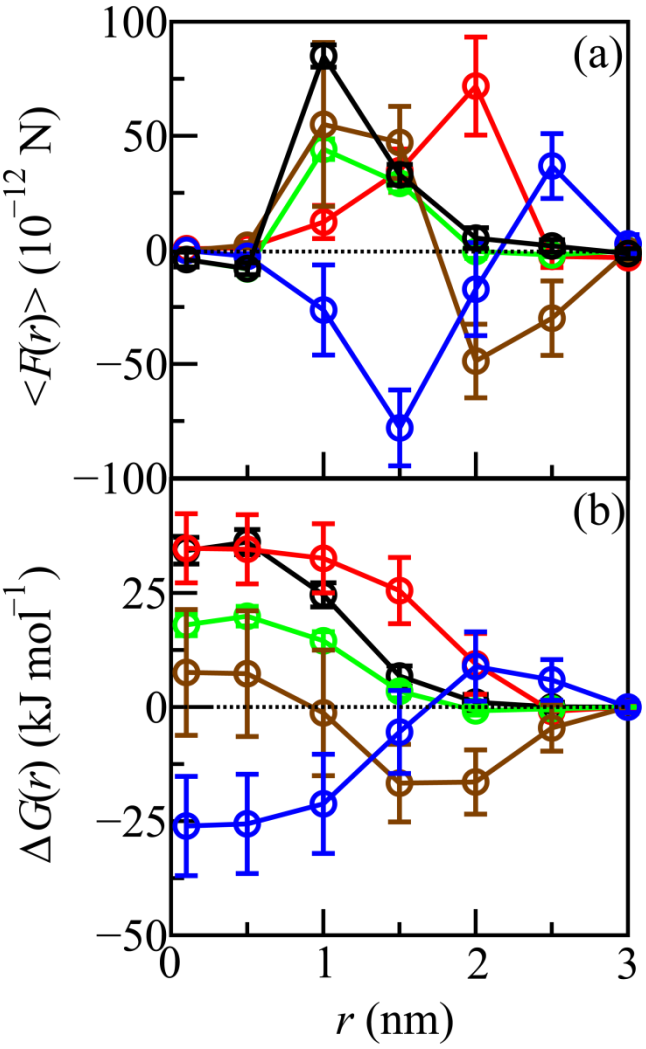

Fig. 5.5 Contributions from hydrophobic groups (○), sulfate ions (○), sodium ions (○), and solvent water (○) to (a) the mean force $\langle F(r) \rangle$ and (b) the free energy profile $\Delta G(r)$ for penetration of water molecules into SDS micelles. ○ represents the total.

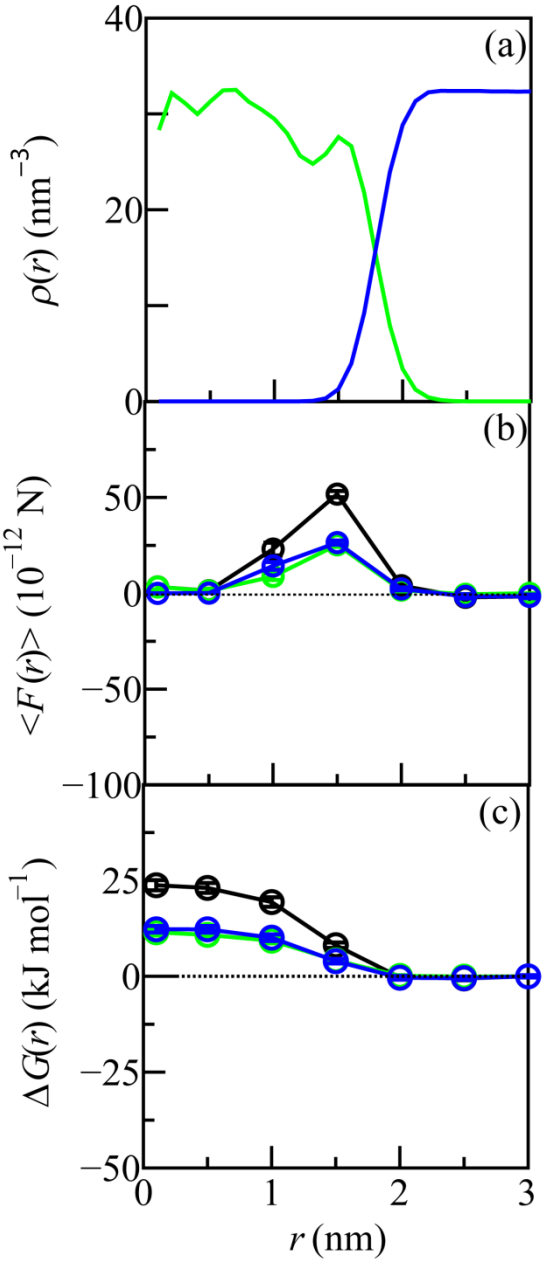

Fig. 5.6 (a) Number density profile of a dodecane droplet solution (—: hydrophobic group; —: water); contributions from hydrophobic groups (○) and solvent water (○) to (b) the mean force <$F(r)$> and (c) the free energy profile $\Delta G(r)$ for transfer of a water molecule into a dodecane droplet. ○ represents the total.

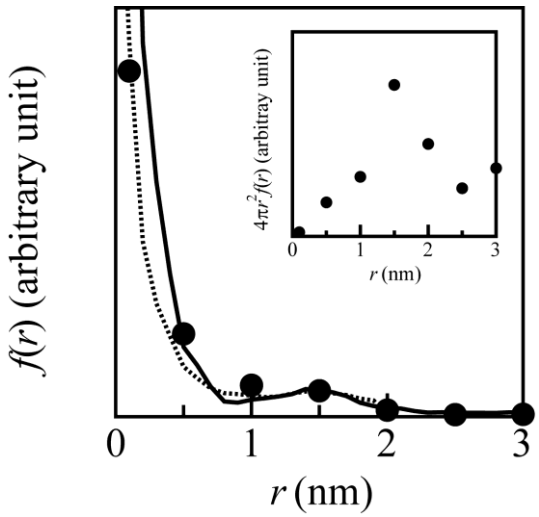

Fig. 5.7 Distribution of methane as a function of radial distance r. ● and ― were calculated from the free energy profile $\Delta G(r)$ and 15-ns MD calculations, respectively. - - - is the distribution of space that can accommodate a sphere of diameter 0.3 nm, i.e., a cavity, in the SDS micelle. All are scaled to the same value at r = 1.5 nm. The density of methane molecules per Cartesian space calculated by multiplying by the Jacobian $4\pi r^2$ is shown in the inset.

REFERENS

1. N. Yoshii, K. Iwahashi, and S. Okazaki J. Chem. Phys., **124**, 184901 (2006).
2. H. F. Huisman, Proc. K. Ned. Akad. Wet., Ser. B: Phys. Sci., **67**, 388 (1964).
3. S. Hayashi and S. Ikeda, J. Phys. Chem. **84**, 744 (1980).
4. P. Lianos and R. Zana, J. Colloid Interface Sci., **84**, 100 (1981).
5. W. L. Jorgensen, J. Chandrasekhar, J. D. Madura, R. W. Impey, and M. L. Klein, J. Chem. Phys., **79**, 926 (1983).
6. A. D. MacKerell, Jr., D. Bashford, M. Bellott, R. L. Dunbrack, Jr., J. D. Evanseck, M. J. Field, S. Fischer, J. Gao, H. Guo, S. Ha, D. J. McCarthy, L. Kuchnir, K. Kuczera, F. T. K. Lau, C. Mattos, S. Michnick, T. Ngo, D. T. Nguyen, B. Prodhom, W. E. Reiher III, B. Roux, M. Schlenkrich, J. C. Smith, R. Stote, J. Straub, M. Watanabe, J. Wiórkiewicz–Kuczera, D. Yin, and M. Karplus, J. Phys. Chem. B, **102**, 3586 (1998).
7. D. MacKerell, Jr., M. Feig, and C. L. Brooks III, J. Comput. Chem., **25**, 1400 (2004).
8. G. J. Martyna, D. J. Tobias, and M. L. Klein, J. Chem. Phys., **101**, 4177 (1994).
9. G. J. Martyna, M. E. Tuckerman, D. J. Tobias, and M. L. Klein, Mol. Phys., **87**, 1117 (1996).
10. G. J. Martyna, M. L. Klein, and M. E. Tuckerman, J. Chem. Phys., **97**, 2635 (1992).
11. U. Essmann, L. Perera, M. L. Berkowitz, T. A. Darden, H. Lee, and L. Pedersen, J. Chem. Phys., **103**, 8577 (1995).
12. N. Matubayasi, K. K. Liang, and M. Nakahara, J. Chem. Phys., **100**, 9025 (2006).
13. A. D. MacKerell Jr., J. Phys. Chem., **99**, 1846 (1995).
14. N. Yoshii and S. Okazaki, Chem. Phys. Lett., **425**, 58 (2006).
15. D. Fincham, N. Quirke, and D. J. Tildesley, J. Chem. Phys., **84**, 4535 (1986).
16. S. Marrink and H. J. C. Berendsen, J. Phys. Chem., **98**, 4155 (1994).
17. W. Shinoda, M. Mikami, T. Baba, and M. Hato, J. Phys. Chem. B, **108**, 4155 (2004).
18. D. Bemporad, J. W. Essex, and C. Luttmann, J. Phys. Chem. B, **108**, 4875 (2004).
19. S. NIhonyangi, S. Yamaguchi, and T. Tahara, J. Am. Chem. Soc., **132**, 6867 (2010)

VI. Free energy of transfer of alcohol and amine from water phase to the micelle by thermodynamic integration method

A. Introduction

In this chapter, in order to clarify the solubilization behavior of solute molecules with alkyl chain and polar groups in the micellar solution, the free energy of transfer of methylamine, octylamine, methanol, and octanol from the water phase to the SDS micelle has been calculated using thermodynamic integration method combined with MD calculations. The influence of the polar group and the length of the alkyl chain on the solubilization is discussed. The binding sites of alkanes, amines, and alcohols in the SDS micelle is also clarified.

B. Molecular dynamics calculation

The aggregation number of SDS micelle was set to 60 for present study since our previous work[1] and as well as light scattering experiments[2, 3] and time-resolved fluorescence spectroscopy[4] indicated that the micelle composed of 60 SDS molecules is thermodynamically most stable in the water. The 60 SDS molecules, 8360 water molecules, and a solute are in a cubic simulation box with periodic boundary condition. Since a critical micellar concentration (CMC) of SDS is 8.1 mM, the concentration of our system corresponds to 50 CMC. TIP4P[5] and CHARMM potential[6, 7] were used for water and other molecules, respectively. The pressure and temperature were controlled at P = 0.1 MPa and T = 300 K using algorithms proposed Martyna *et al*[8, 9]. Inertial constant of the barostat was set to 6.7×10^{-17} J s^2 such that the relevant time constant is 2.0 ps. Nosé-Hoover chain thermostat of five chains was connected to particle degrees of freedom and barostat, separately. Inertial constants of the thermostat for the former were set to 3.6×10^{-21} J s^2 for the first chain and 1.2×10^{-21} J s^2 for the second to fifth chains and those for the latter to 4.2×10^{-18} J s^2 for the first chain and 7.5×10^{-23} J s^2 for the

second to fifth chains. Time constant of the five chains are all 0.5 ps.[8, 10] The time step, Δt, was set to be 2 fs. The particle mesh Ewald (PME) method was used in order to calculate the Coulomb interaction. The cutoff distance for Lennard-Jones interaction and the real space of PME method was 1 nm. The parameter α and the grid points of PME method were 0.4×10^{10} m^{-1} and $64 \times 64 \times 64$, respectively[11]. SHAKE/ROLL and RATTLE/ROLL methods were used to constrain the bond length between heavy atoms (carbon, oxygen, and nitrogen) and hydrogen (H) atoms in dodecyl sulfate (DS) ions, the solute and water. Those methods were also used in order to constrain the bending angles H–C–H in methylene groups, H–O–H in the water molecule and H-N-H in the amine.

The suitable sets of the coupling parameters (λ_1, λ_2) were selected in order to evaluate the integrals of Eq. (2.7) with high accuracy. For two small solutes (methylamine and methanol molecules) 1-ns molecular dynamics calculations have been performed at 12 sets of λ: (λ_1, λ_2) = (0, 0), (0, 0.05), (0, 0.1), (0, 0.2), (0, 0.3), (0, 0.4), (0, 0.5), (0.2, 0.6), (0.4, 0.7), (0.6, 0.8), (0.8, 0.9), and (1, 1). For long solutes (octanol and octylamine molecules) 1-ns MD calculations have been also performed at 2 sets, (λ_1, λ_2) = (0, 0.01) and (0.025), in addition to the previous twelve (λ_1, λ_2) sets. The first 0.5-ns trajectory was excluded from the analysis.

In order to obtain trajectory of solute in the SDS micellar solution and calculate the radial distribution of it in the micelle (see in subsection VI.C.3), another 15-ns MD calculations have been also performed without wall potential $\varphi_{\mathrm{wall}}(R, R_{\mathrm{m}})$. The simulation box has 60 SDS molecules, 8 360 water molecules, and one solute (methylamine, octylamine, methanol, or octanol). The other calcula-

tion conditions were the same as the above-mentioned free energy calculations. The last 10-ns trajectory was used for analysis.

C. Results and discussion

Figure 6.1 shows $\partial V/\partial\lambda_2$ in Eq. (2.7) and its cumulative average of octylamine as a function of time at $\lambda_1 = 0$ and $\lambda_2 = 0.05$, where convergence of cumulative average of $\partial V/\partial\lambda_2$ is the slowest and an error of $\langle \partial V/\partial\lambda_2 \rangle_{\lambda_1,\lambda_2}$ is the largest among the all sets of $\boldsymbol{\lambda}$. Dashed line in Fig. 6.2 indicates the average value obtained from the 0.5-ns MD calculation. As shown in the figure, the cumulative average converged well, and the 0.5-ns MD calculation is long enough to obtain satisfactory statics for the integrand of Eq. (2.7). As a result, it is possible to calculation numerically the integral of Eq. (2.7) with satisfactory accuracy.

1. *Excess free energy of transfer from ideal gas state to the water phase and to the SDS micelle*

Excess free energy of transfer of methylamine, octylamine, methanol, and octanol from ideal gas state to the water phase, $\Delta G^{ex}_{id\rightarrow w}$, and to the SDS micelle, $\Delta G^{ex}_{id\rightarrow m}$, has been calculated by numerical integration according to Eq. (2.7). Obtained $\Delta G^{ex}_{id\rightarrow w}$ and $\Delta G^{ex}_{id\rightarrow m}$ are shown in Fig. 6.2 as an energy level diagram. In Fig. 6.2 blue and red lines represent $\Delta G^{ex}_{id\rightarrow w}$ and $\Delta G^{ex}_{id\rightarrow m}$, respectively. Solid circles are hydration free energy obtained by solubility experiments of these molecules in pure water.[12] It is interesting that $\Delta G^{ex}_{id\rightarrow w}$ is in good agreement with the experimental hydration free energy despite difference between the water phase in the micellar solution and pure water. For instance, calculated $\Delta G^{ex}_{id\rightarrow w}$ of octanol is – 14 ± 3 kJ mol^{-1}, and the corresponding experimental value is -17 kJ mol^{-1}. Within the error these values agree well with each other. The other solutes also show the sim-

ilar result. The solutes are considered to interact weakly with sodium ions in the water phase.

$\Delta G^{ex}_{id\rightarrow w}$ of hydrophobic methane and octane molecules are 9.8 and 15 kJ mol^{-1}, respectively. These molecules are less stable in the water phase than in the ideal gas state because of hydrophobic hydration. On the other hand, $\Delta G^{ex}_{id\rightarrow w}$ of methylamine, octylamine, methanol, and octanol molecules which also have hydrophilicity are – 15, – 21, – 12, and – 14 kJ mol^{-1}, respectively, i.e., negative values. It is because hydrogen-bonding is formed between the polar amine or hydroxyl group and solvent water that these solutes are more stable in the water phase than in the ideal gas state.

Comparing octyl group with methyl one, $\Delta G^{ex}_{id\rightarrow w}$ of octyl one is 3−7 kJ mol^{-1} larger than that of methyl one. Increase of the alkyl chain length causes the larger hydrophobic hydration in the water phase, and has a influence on the stability of the solutes, though the instability is not so large compared with the $\Delta G^{ex}_{id\rightarrow m}$ stated below.

Concerning $\Delta G^{ex}_{id\rightarrow m}$, methane has a positive value (4.4 kJ mol^{-1}), and is unstable in the SDS micelle. In contrast, $\Delta G^{ex}_{id\rightarrow m}$ of the other solutes is negative value. These molecules are 17−22 kJ mol^{-1} more stable in the SDS micelle than in the ideal gas state with increasing the number of carbon atoms. It is the opposite behavior to $\Delta G^{ex}_{id\rightarrow w}$. Increase of the alkyl chain leads to stronger interaction between the alkyl chains of the solutes and hydrophobic core of SDS micelle.

2. *Stability and binding ratio of solutes in the SDS micelle*

In this subsection, we discuss the stability of the solutes between in the SDS micelle and in the water phase. Table 6.1 lists the free energy, $\Delta G_{w\rightarrow m}$, of transfer from the water phase to the SDS

micelle. Here, it is noted that $\Delta G_{w\to m}$ obtained by Eq. (2.12) includes the ideal term of the free energy calculated as a function of the ratio of volume of the SDS micelle(V_m) to that of the water phase(V_w). In this paper, concentration of SDS in the simulation box is corresponding to 50 CMC. The value of $k_B T \ln \frac{V_m}{V_w}$ is, then, 1.8 kJ mol^{-1}.

From $\Delta G_{w\to m}$ in Table 1, the solutes except for methanol are more stable in the SDS micelle than in the water phase. This indicates that the alkyl chain of the solutes interacting with the micelle core is more stable than that in the water phase with hydrophobic hydration. This tendency is clearly shown in the case with long alkyl chain. The difference of the $\Delta G_{w\to m}$ becomes 23−26 kJ mol^{-1} for octyl group.

On the other hand, in the case with short alkyl chain i.e. methyl group the stability of the solutes in the SDS micelle is relatively small. For example, $\Delta G_{w\to m}$ of methylamine and methanol are -1.2 ± 4 and +0.8 ± 3 kJ mol^{-1}, respectively, so that these molecules may be more stable in the water phase than in the SDS micelle. This hydrophilic nature of methylamine and methanol is the result of hydrophilicity of amine and hydroxyl groups is comparable to hydrophobicity of methyl group.

The gradient of $\Delta G_{w\to m}$ of amine or alcohol as function of the number of carbons is 3 kJ mol^{-1}. This value is in good agreement with the gradient of alkane (3.3 kJ mol^{-1}). This result indicates that alkyl chain length of the solute is important for the stabilization of the solute in the micelle.

The difference, $\Delta\Delta G_{w\to m}$, of the $\Delta G_{w\to m}$ between alkane and amine or alcohol with the same carbon chain lengths as alkane is listed in Table 6.1. $\Delta\Delta G_{w\to m}$ of methanol is almost equal to

that of the methylamine. Similarly, $\Delta\Delta G_{w\to m}$ of octanol is similar to that of octylamine. These results indicate that hydrophilicity of hydroxyl group is almost equal to that of amine group. This is due to high hydrogen bonding capacity of alcohol and amine caused by a large electron negativity of oxygen and nitrogen atoms. This high hydrophilicity affects binding ratio of the solute to the micelle.

The binding ratio of the solutes in the SDS micelle to that in the water phase is also listed in Table 6.1. Here, the binding ratio is evaluated from $\exp\left(-\Delta G_{w\to m}/RT\right)$, where R and T are gas constant and absolute temperature, respectively. The binding ratio of small solutes (methane, methylamine, and methanol) is small value between 0.7 and 4. Those molecules are considered to be widely distributed in the whole region of the micellar solution i.e., both in the micelle core and in the water phase. On the other hand, the binding ratio of the long solutes such as octane, octylamine, and octanol is several tens of thousands, so that those molecules may penetrate into the SDS micelle and are localized there because of the hydrophobic nature of the long alkyl chain.

3. *Distribution of the solutes*

In order to clarify where the solutes are bound to the SDS micelle, the radial distribution of each solute in the SDS micellar solution is calculated using the trajectory of 15-ns MD run without wall potential (see section VI.B). The radial distribution $f(R)$ of the hydrophobic part and sulfate ion of SDS micelle, sodium ion, and water molecule are shown as a function of the distance, R, from the center of mass of the SDS micelle in Fig. 6.3(a). The radial distribution, f(R), of alkane, amine, and alcohol is also shown as a function of R in Fig. 6.3(b), (c), and (d), respectively. Each $f(R)$ was obtained from the number density profile $\rho(R)$ of the solute divided by Jacobian $4\pi R^2$:

$f(R) = \rho(R) / 4\pi R^2$. Then, $f(R)$ should be in proportion to $\exp -\Delta G^{ex}_{w\to m} / RT$. (It is noted that $\rho(R)$ is in proportion to $\exp -\Delta G_{w\to m} / RT$.) The red and black lines in the Fig. 6.3(b), (c), and (d) of methyl and octyl groups in the solutes, respectively. The solid and dotted lines are $f(R)$ of hydrophobic carbon chain and hydrophilic group, respectively.

As shown in Fig. 6.3(b), methane and octane molecules are more distributed in the SDS micelle than in the water phase. In particular, binding probability increases in the vicinity of the center of mass of the SDS micelle, where the density of the hydrophobic part is low enough.

In the water phase, $f(R)$ for methane is small, and that for the octane is almost 0. $\Delta G^{ex}_{w\to m}$ of methane is – 5.4 kJ mol^{-1}, only twice as large as thermal fluctuation energy (2.5 kJ mol^{-1}) at T = 300 K, so that methane can be distributed in the water phase. On the other hand, octane has a large value, − 28 kJ mol^{-1}, and is localized and stabilized in the vicinity of the SDS micelle core to avoid contact with solvent water molecules.

Figure 6.3(c) shows the radial distribution $f(R)$ of methyl- and octylamine. Methylamine is distributed in the vicinity of the surface of the SDS micelle ($1 \leq R \leq 2$ nm). This binding of methylamine can be considered as a result of the competition between the hydrophilicity of the polar amine group and the hydrophobicity of the non-polar methyl group. Furthermore, methylamine easily go to the water phase, since $\Delta G^{ex}_{w\to m}$ of methylamine is – 3 kJ mol^{-1}, and is as small as the thermal fluctuation energy. In contrast, for the octylamine the alkyl chain of octylamine is buried in the hydrophobic part of the SDS micelle to avoid hydrophobic hydration, whereas the amine group keeps on forming of

the hydrogen-bonding with solvent water molecules. Thus, the octylamine is solubilized in the SDS micelle with palisade layer structure.

Figure 6.3(d) shows the radial distribution $f(R)$ of methanol and octanol as a function of R. Methanol is distributed in the whole region of the micellar solution from the hydrophobic part of the micelle to the water phase. Though some methanol molecules are bound to the micelle, $\Delta G^{ex}_{w\rightarrow m}$ of methanol molecule is – 1 kJ mol^{-1}, and is half of the thermal fluctuation energy (2.5 kJ mol^{-1}) at T = 300 K, so that methanol can dissolve into the water phase and move about in the whole region of the micellar solution. As shown in the figure, methanol slightly penetrates into the SDS micelle. On the other hand, the alkyl chain of octanol is buried in the hydrophobic SDS micelle core as well as octylamine to avoid the hydrophobic hydration. Octanol is, then, solubilized in the SDS micelle with the palisade layer structure.

D. Conclusion

The free energy of transfer of methylamine, octylamine, methanol, and octanol from the water phase to the SDS micelle has been calculated by MD calculation. The calculated free energy was compared with that of alkanes obtained by our previous work. In contrast to the hydrophobic methane and octane, methylamine, octylamine, methanol, and octanol are stable in the water phase since these molecules have a polar group.

The methane is unstable in the SDS micelle due to gaseous matter at ambient condition. On the other hand, from the free energy $\Delta G_{\mathrm{w}\to\mathrm{m}}$ of transfer obtained by Eq. (2.12), all the solutes except for the methanol and methylamine were found to be stable in the SDS micelle. With increasing the alkyl chain length, the solute is more stable in the SDS micelle. Stability of the solutes is in order of alkane > amine ≈ alcohol. The methanol and methylamine were stable in the water phase as well as in the SDS micelle at 50 CMC because of their high hydrophilicity. The binding ratio of small solutes such as methane, methylamine, and methanol in the SDS micelle is small value between 0.7 and 4. In contrast, that of large solutes such as octane, octylamine, and octanol is several tens of thousands.

The radial distribution of methane, octane, methylamine, octylamine, methanol, and octanol has been evaluated as a function of the radial distance, *R*, from the center of mass of SDS micelle to the solutes. The methane and octane molecules can be found in the SDS micelle core. $\Delta G^{\mathrm{ex}}_{\mathrm{w}\to\mathrm{m}}$ of methane is, however, small so that the methane may go in and out the SDS micelle. The methylamine was adsorbed on the SDS micelle surface. The methanol moves about from the surface of SDS micelle

to the water phase since $\Delta G^{ex}_{w\rightarrow m}$ of the methanol molecule is – 1 kJ mol^{-1} half as high as thermal fluctuation energy (2.5 kJ mol^{-1}) at T = 300 K. The octylamine and octanol are solubilized in the SDS micelle with palisade layer structure.

TABLE 6.1 the total free energy, $\Delta G_{w\to m}$, of transfer from the water phase to the SDS micelle obtained by Eq. (2.12)and the difference $\Delta\Delta G_{w\to m}$ between $\Delta G_{w\to m}$ of the alkanes and that of the amines or alcohols with the same carbon chain length as the alkane. The binding ratio of the solute in the SDS micelle to that in the water phase was calculated by $\exp\left(-\Delta G_{w\to m}/RT\right)$. R and T are gas constant and absolute temperature, respectively. H, NH_2, and OH represent alkane, amine, and alcohol, respectively. The error of methane and octane are re-evaluated using our previous data[18]. The error in present work represents 80% confidence interval.

	Methyl groups			Octyl groups		
	H	NH_2	OH	H	NH_2	OH
$\Delta G_{w\to m}$ /kJ mol^{-1}	− 3.6 ± 1	− 1.2 ± 4	+ 0.8 ± 3	− 26 ± 2	− 26 ± 8	− 23 ± 6
$\Delta\Delta G_{w\to m}$ /kJ mol^{-1}	-	+ 3.8 ± 4	+ 4.4 ± 3	-	0 ± 8	+3 ± 6
The ratio	4	1	0.7	30 000	30 000	10 000

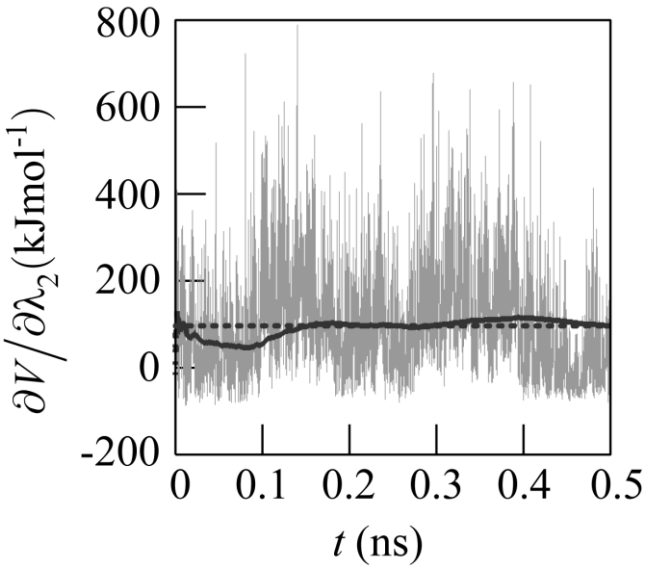

Fig. 6.1 $\partial V/\partial\lambda_2$ in Eq. (2.7)of the octylamine at $\lambda_1 = 0$ and $\lambda_2 = 0.05$ as a function of time (gray line) as well as its cumulative average (black line). Dashed line is total average.

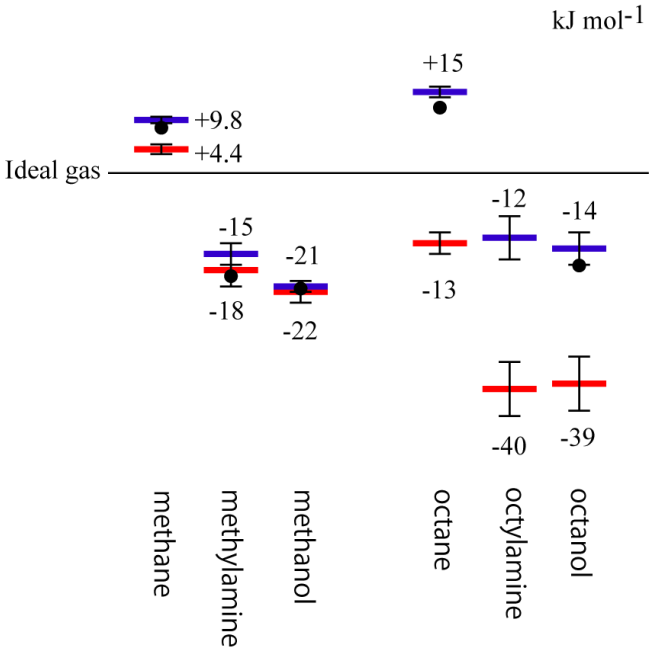

Fig. 6.2 The calculated free energy level for methane, octane, methylamine, octylamine, methanol, and octanol molecules in the water phase (blue) and in the SDS micelle (red). Solid circle is the experimental hydration free energy.

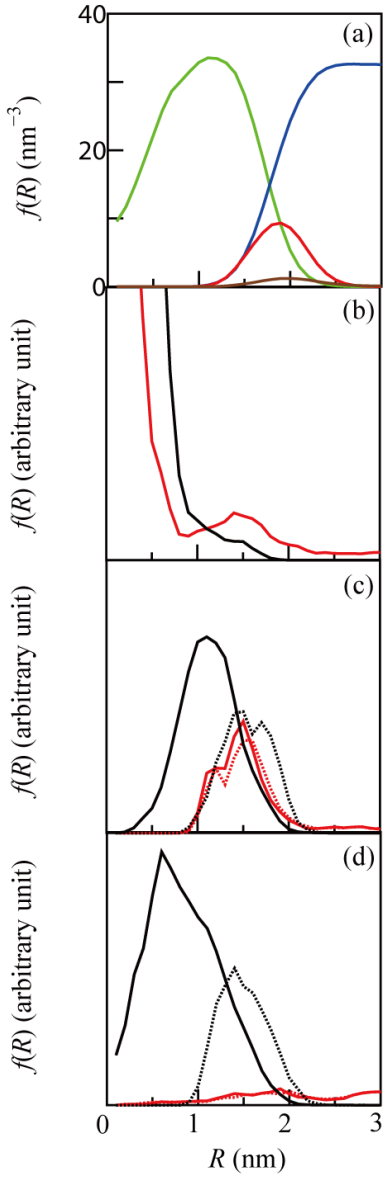

Fig. 6.3 (a) Radial distribution $f(R)$ of SDS micelles as a function of radial distance R from the center of mass of the SDS micelle (green: hydrophobic carbon atom, red: sulfur and oxygen atom of sulfate ion, blue: water molecule, and brown: sodium ion). Radial distribution $f(R)$ of alkane (b), amine (c), and alcohol (d) as a function of radial distance R from the 15-ns MD calculations. The red and black lines represent $f(R)$ of methyl and octyl groups in the solutes, respectively. The solid and dashed lines are $f(R)$ of hydrophobic carbon chain and hydrophilic group, respectively.

REFERENCE

1. N. Yoshii, K. Iwahashi, and S. Okazaki J. Chem. Phys. **124,** 184901 (2006).

2. H. F. Huisman, Proc. K. Ned. Akad. Wet., Ser. B: Phys. Sci. **67**, 388 (1964).

3. S. Hayashi and S. Ikeda, J. Phys. Chem. **84**, 744 (1980).

4. P. Lianos and R. Zana, J. Colloid Interface Sci. **84**, 100 (1981).

5. W. L. Jorgensen, J. Chandrasekhar, J. D. Madura, R. W. Impey, and M. L. Klein, J. Chem. Phys. **79**, 926 (1983).

6. A. D. MacKerell, Jr., D. Bashford, M. Bellott, R. L. Dunbrack, Jr., J. D. Evanseck, M. J. Field, S. Fischer, J. Gao, H. Guo, S. Ha, D. JosephMcCarthy, L. Kuchnir, K. Kuczera, F. T. K. Lau, C. Mattos, S. Michnick, T. Ngo, D. T. Nguyen, B. Prodhom, W. E. Reiher III, B. Roux, M. Schlenkrich, J. C. Smith, R. Stote, J. Straub, M. Watanabe, J. Wiórkiewicz-Kuczera, D. Yin, and M. Karplus, J. Phys. Chem. B **102**, 3586 (1998).

7. A. D. MacKerell, Jr., M. Feig, and C. L. Brooks III, J. Comput. Chem. **25** 1400 (2004).

8. G. J. Martyna, D. J. Tobias, and M. L. Klein, J. Chem. Phys. **101**, 4177 (1994).

9. G. J. Martyna, M. E. Tuckerman, D. J. Tobias, and M. L. Klein, Mol. Phys. **87**, 1117 (1996).

10. G. J. Martyna, M. L. Klein, and M. E. Tuckerman, J. Chem. Phys. **97**, 2635 (1992).

11. U. Essmann, L. Perera, M. L. Berkowitz, T. A. Darden, H. Lee, and L. Pedersen, J. Chem. Phys. **103**, 8577 (1995).

12. S. Cabani, P. Gianni, V. Mollica, and L. Lepori, J. Solution Chem. **10**, 563 (1981)

VII. Conclusion

In order to obtain atomic-level information of thermal stability and a binding sites of solutes in the micelle, physicochemical study of solubilization has been performed by molecular dynamic calculations.

Free energy of transfer of a series of alkane, i.e. methane, ethane, butane, pentane, hexane, and octane as well as amphiphilic molecules such as methylamine, octylamine, methanol, and octanol, from water phase to SDS micelle, has been calculated using thermodynamics integration methods combined with molecular dynamics calculations. The obtained free energy of transfer of alkanes was divided into the enthalpic and entropic contributions. Free energy profile for penetration of methane and water molecules from water phase to SDS micelles has also been calculated.

In chapter III, free energy of transfer of a series of alkane, i.e. methane, ethane, butane, pentane, hexane, and octane from water phase to SDS micelle has been calculated using thermodynamics integration methods combined with molecular dynamics calculations. The free energy of transfer of all alkanes was negative values, that is, the alkanes in the SDS micelle are more stable than in the water phase in order to avoid the alkanes contacting with water molecule. Further, The calculated free energy of transfer decreases almost linearly as a function of the number of carbon atoms of the alkanes with a decrement of 3.3 kJ mol^{-1} per one methylene group. The calculated free energy of transfer indicates that at the micelle concentration of 50 CMC, about only 1 of 6 micelles or 1 of 32,000 micelles does not contain a solute methane or n-octane molecule, respectively.

In chapter IV, the free energy of transfer was divided to enthalpy and entropy. The entropy

and enthalpy decreases linearly as a function of the number of carbon atoms of the alkanes. Structural behavior of the solubilized alkane molecules in the micelle has been analyzed, too. The longer the alkane is, the more localize its spatial distribution is in the micelle core. The conformations of n-octane in the micelle and water phase have been analyzed. The octane molecule has more compact conformation in the water phase to reduce the contact with water, resulting in a wide distribution. In the micelle core, however, n-octane has a stretched structure to fit the linear alkyl chain of dodecyl sulfate ion.

In chapter V, the free energy profiles for penetration of methane and water molecules into SDS micelles have been calculated as a function of distance *r* from the SDS micelle to the methane and water molecules. No free energy barrier is observed in the vicinity of the sulfate ions of the SDS micelle, implying that methane is easily drawn into the SDS micelle. The methane may move about in the SDS micelle. On the other hand, the free energy of water molecule has a large positive value, so that the water molecule can not be penetrated into SDS micelle. Based on analysis of the contributions from hydrophobic groups, sulfate ions, sodium ions, and solvent water to the free energy for penetration, the methane molecule is dissolved by hydrophobic effect. These contributions to the penetrating water molecule change in complex ways as a function of *r*, and cancel one another, so that the contribution of hydrophobic part of SDS micelle is major reason for not penetrating of water to SDS micelle. Finally, the radial distribution of solubilized methane has been evaluated from $\exp\{-\Delta G(r)/RT\}$. A good correlation was found between the radial distribution of cavities in the SDS micelle with 0.3 nm diameter and that of the methane. The methane is considered not to be localized and to move about in

the SDS micelle using cavities in the hydrophobic core. It is interesting to find that after the volume factor Jacobian $4\pi r^2$ is taken into account, the methane is most often observed in the interface.

In chapter VI, the free energy of transfer of methylamine, octylamine, methanol, and octanol from the water phase to the SDS micelle has been calculated by MD calculation in addition to the one of methane and octane. The calculated excess free energy shows that the molecules are all stable in the SDS micelle. The longer the alkyl chains in the penetrating molecules are, the more stable the penetrating molecules in the SDS micelle. However, the methanol was more stable in the water phase than in the SDS micelle at 50 CMC when the ideal term is also taken into account. The ratio of the probability that we find methane, methylamine, and methanol in the SDS micelle to that we find them in the water phase is small rangy from 0.7 to 4. On the other hand, that of octane, octylamine, and octanol is several tens of thousands. The distribution of methane, octane, methylamine, octylamine, methanol, and octanol has been evaluated as a function of distance, *R*, from the center of mass of SDS micelle to the penetrating molecule by 15 ns-long MD calculations. The methane and octane molecule are found in the SDS micelle core. The methylamine was adsorbed on the SDS micelle surface. The methanol is found everywhere in the system from the surface of SDS micelle to the water phase. The octylamine and octanol are solubilized in the SDS micelle with palisade layer structure.

In the present study it is clarified that the binding sites and binding strength of the penetrating molecules with micelles can be evaluated by atomic-level molecular dynamics calculations. Further, we can obtain the intermolecular interactions which promote or inhibit the solubilization of the

penetrating molecules. Such information is very important to control the character of products in various fields such as cosmetics, manufacturing pharmacy, etc. We believe that our research contributes much to the molecular design of the products.

Acknowledgments

I would like to acknowledge Prof. S. Okazaki for his valuable discussion and guidance during the course of this work. I am also grateful to Dr. N. Yoshii for his encouragement and valuable discussion. I give my thanks to Dr. A. Yamada and Y. Andoh for their discussion and encouragement. I would like to express my thanks to all members of Okazaki group.

I thank the Okazaki Research Center for Computational Science, National Institute of Natural Science, the Center for Computational Science, University of Tsukuba, and the Information Technology Center of Nagoya University for the use of supercomputers.

I thank Iue Memorial Foundation for financial support.

List of Publications

The content of this thesis is composed of following papers;

Chapter III.

- Molecular dynamics study of solubilization of immiscible solutes by a micelle: Free energy of transfer of alkanes from water to the micelle core by thermodynamic integration method
  K. Fujimoto, N. Yoshii, and S. Okazaki, J. Chem. Phys. **133**, 074511 (2010)

Chapter IV.

- Enthalpy and entropy of transfer of alkanes from water phase to the micelle core
  K. Fujimoto, N. Yoshii and S. Okazaki, Mole. Sim., in press.

Chapter V.

- Free energy profiles for penetration of methane and water molecules into spherical sodium dodecyl sulfate micelles obtained using the thermodynamic integration method combined with molecular dynamics calculations
  K. Fujimoto, N. Yoshii, and S. Okazaki, J. Chem. Phys., **136,** 041511 (2012).

Chapter VI

- Molecular dynamics study of penetration of solutes into a micelle: Free energy of transfer of alcohol and amine from water phase to the micelle by thermodynamic integration method
  K. Fujimoto, N. Yoshii, and S. Okazaki, in preparation.